

1 **Author's response to referee 1:**

2 Thank you very much for your constructive comments! You helped us improve this study significantly.

3 1) Main Comments: lines 403 – 406 and Table 5 The effect of the SOC on the gross uptake flux seems too  
4 large (Table 5). A note confirming this has been added in this version of the manuscript (lines 403 – 406)  
5 but there is still no explanation given. The 30% extra SOC increases the gross production, which makes  
6 more CO available in the soil, which in turn leads to an increase in the gross CO consumption from the  
7 soil. But, for an increase in SOC of 30%, the production increases by about 10Tg/year, and the gross  
8 consumption increases by 28 Tg/year! This means that an extra 18 Tg /year is taken from the  
9 atmosphere. I do not understand how this happens, as I think an increase in soil CO concentration  
10 cannot lead to an increase in the uptake of CO from atmosphere. (An increase of uptake from the  
11 atmosphere would actually need a decrease in the CO concentration in the upper layer of soil.) Also,  
12 from Eq. 2.x, it is clear that the uptake is related to SOC only via the CO soil concentration.  
13 Please explain and/or correct if this is an error.

14 **Response: Thank you for pointing this out. We have double checked the sensitivity results and found**  
15 **the extra 18 Tg CO yr<sup>-1</sup> from air to soils is due to current time step (5min) in combination with sudden**  
16 **a 30% SOC increase. To explain this, we have tested the model using different time steps and SOC**  
17 **increasing percentages. In this revision, we have added a new table (Table 7) to show the test results**  
18 **and discussed this issue in Section 4.3 and lines 452 to 462: “Fourth, from sensitivity test (Table**  
19 **5) and model test (Table 7), we notice that the diffusion and consumption in the model**  
20 **is very sensitive to sudden 30% SOC changes with 5-minute time step. In reality,**  
21 **diffusion and consumption shall only be slightly influenced by indirect changes of soil**  
22 **CO concentration due to SOC changes. When we used 3-minute or 1-minute time step,**  
23 **the model responses to SOC changes are reasonable (Table 7). However, we believe**  
24 **5-minute step is suitable in this study since SOC varies slightly during the whole global**

25 simulation period with only 3% increasing from 1900 to 2013 (Figure 4d) and up to a 4%  
26 increase from 2014 to 2100 (Figure 6g). Our model test showed there are small  
27 responses to these small amounts of SOC increasing (Table 7).”

28

29

30 **Technical and text comments**

31 2) line 23: CO deposition velocity – net or gross?

32 **Response: It is “net” deposition velocity. We have corrected in line 23.**

33

34 3) line 25: why will deposition velocity increase? which are the main factors? Add a short explanation,  
35 e.g. “mainly due to xxx” xxx = increase in temperature?

36 **Response: We have added explanation at the end in lines 24 to 27. “Under the future climate**  
37 **scenarios, the CO deposition velocity will increase at 0.0002-0.0013 mm s<sup>-1</sup> yr<sup>-1</sup> during 2014-2100,**  
38 **reaching 0.20-0.30 mm s<sup>-1</sup> by the end of the 21st century, primarily due to increasing temperature.”**

39

40 4) line 54: since you just shown negative values, I think it is better to specify here what are the negative  
41 fluxes, e.g. (negative values represent deposition from atmosphere to soil)

42 **Response: We have revised the sentence based on your suggestion in line 54. “negative values**  
43 **represent the uptake from the atmosphere to soil”**

44

45 5) lines 55 – 56: “All existing estimates have large uncertainties ranging from -16 to -640 Tg CO yr<sup>-1</sup>” is  
46 this the range for estimates, or for uncertainties? – unclear, please reformulate

47 **Response: We have reformulated the sentence based on your comment in lines 55 to 56. “All existing**  
48 **estimates have large uncertainties and range from -640 to -16 Tg CO yr<sup>-1</sup>”**

49

50 6) lines 56 – 57: “the estimates of CO dry deposition velocities also have large uncertainties, ranging  
51 from 0 to 4.0mm s<sup>-1</sup>” – is this the range for estimates, or for uncertainties? – unclear, please  
52 reformulate

53 **Response: We have reformulated the sentence based on your comment in lines 57 to 58. “Similarly,**  
54 **the estimates of CO dry deposition velocities also have large uncertainties and range from 0 to 4.0mm**  
55 **s<sup>-1</sup>”**

56  
57 7) lines 145 – 147: I think a piece of text is missing here. D is calculated using the method of Potter.  
58 Equations 2 – 4 are not related to D, but to the production and consumption rates P and O. Please check.

59 **Response: Thank you for pointing this out. This is a mistake. We have removed this from line 146.**

60  
61 8) from line 155 till the end of this section: it is unclear what some of the numbers represent. E.g. why  
62 V<sub>max</sub> is a range and not one value? It would be good to explain here shortly that V<sub>max</sub> (also other  
63 parameters) are ecosystem specific, and that’s why there are multiple values. This is shown later in Sect  
64 2.3 but not clear here.

65 Also, are the V<sub>max</sub> values taken from Whalen & Reeburgh, 2001, or optimized in this work? If they are  
66 optimized in this work (as described in Sect. 2.3) then remove the reference to Whalen & Reeburgh (line  
67 156). The same for kCO, and all the parameters optimized in this work – the way some of the references  
68 are given now suggests that the values are taken from those papers.

69 **Response: Thank you for pointing this out. They are observed or estimated values from previous**  
70 **studies, which will be used as a prior during our parameterization. We have added explanations for**  
71 **this in lines 154 to 156. “Where V<sub>max</sub> is the ecosystem-specific maximum oxidation rate and was**  
72 **estimated previously ranging from 0.3 to 11.1 µg CO g<sup>-1</sup> h<sup>-1</sup> for different ecosystems (Whalen &**

73 **Reeburgh, 2001)”. And lines 165 to 166, “and their values were previously estimated ranging from 5 to**  
74 **51  $\mu\text{l CO l}^{-1}$  for different ecosystems (Whalen & Reeburgh, 2001)”**

75

76 9) lines 210 – 211: “uptakes”, “depositions” and “emissions” should be “uptake”, “deposition” and  
77 “emission”

78 **Response: We have corrected this. Please see lines 211 to 212. “Positive values of  $v_d$  are soil uptake**  
79 **(deposition from air to soils) and negative values are soil emissions.”**

80

81 10) line 260: I suggest to state here explicitly that the CO surface concentration is constant in time.

82 **Response: We have revised the sentence based on your comment in lines 262 to 263. “to calculate the**  
83 **distribution of static CO surface concentrations”**

84

85 11) lines 314 – 315: I think the ranges should be given with the lower value first, e.g. “-180 to -197”  
86 should be “-197 to -180”; same for -145 to -163. Same for the following: abstract; lines 373 – 374, 483

87 **Response: Thank you for your suggestion. We have revised all places through the manuscript to use**  
88 **values lower value first. Please see lines 16 to 17, line 53, line 56, lines 315 to 315, line 336, line 374 to**  
89 **375, line 383, and lines 492.**

90

91 12) lines 343 – 345: Fig. 9 does not show consumption, production and net flux

92 **Response: Thank you for pointing this out. We have corrected this sentence in lines 344 to 345.**  
93 **“During 2014-2100, there are significant trends of increasing deposition velocities for nearly all**  
94 **scenarios (Figure 9).”**

95

96 13) line 351: replace “from RCP2.6 to 8.5” by “from RCP2.6 to RCP8.5”

97 **Response: We have corrected this in line 352. “Deposition velocities are increasing from RCP2.6 to**  
98 **RCP8.5 and larger than in the historical periods in areas near the equator (Figure 10).”**

99

100 14) line 355: Table 5 should be Table 4

101 **Response: We have corrected this in lines 355 to 356. “Different vegetation types have a large range**  
102 **of deposition velocity, from 0.008 to 1.154 mm s<sup>-1</sup> (Table 4).”**

103

104 15) lines 450 – 452: What is meant here by “derived CO concentration”? – is it the constant, latitude  
105 dependent CO derived with the function 5? Please clarify. Also, if this is the case, a lower than real CO  
106 concentration will lead to an underestimation of CO deposition, and not to an overestimation, correct?

107 **Response: Thank you for pointing this out. We have rewritten the sentence and corrected to**  
108 **“underestimation” in lines 450 to 452. “Third, the static CO surface concentration derived from the**  
109 **empirical function is lower than MOPITT CO surface concentration, which will lead to underestimation**  
110 **of CO deposition velocity during 1901-2100.”**

111

112 16) Table 5 – please check the sign of the % values. I think for Consumption and Net flux all the % values  
113 have the wrong sign. E.g. the change in consumption from baseline to (CO + 30% ) should be + 11% (-  
114 164.14 - (-147.65) / (-147.65) = 11.17).

115 **Response: Thank you for pointing out this mistake. We have made corrections in Table 5.**

116

117 17) Fig. 3. I find it difficult to see some of the plots, in particular the measurement data in plots a2 and  
118 c2. Also the x-axis labels of a1, b1, c1 and d1 are difficult to see at normal page zoom.

119 **Response: We have re-plotted the figure using two times bigger symbol for measurement data in**  
120 **Figures 3a2, 3b2, 3c2 and 3d2. Also we have used two times bigger x-axis label for Figures 3a1, 3b1,**  
121 **3c1, and 3d1. Please see Figure 3.**

122

123 18) Fig. 9 caption: remove the first "Future"

124 **Response: We have removed it.**

125

126 19) Fig. 12. typo in all x-axes labels, should be "concentration"

127 **Response: We have corrected the x-axis labels for figure 12.**

128

**Global Soil Consumption of Atmospheric Carbon Monoxide:  
An Analysis Using a Process-Based Biogeochemistry Model**

Licheng Liu<sup>1</sup>, Qianlai Zhuang<sup>1,2</sup>, Qing Zhu<sup>1,3</sup>, Shaoqing Liu<sup>1,4</sup>, Hella van Asperen<sup>5</sup>, Mari  
Pihlatie<sup>6,7</sup>

<sup>1</sup>Department of Earth, Atmospheric, Planetary Sciences, Purdue University, West Lafayette, IN 47907,  
USA

<sup>2</sup>Department of Agronomy, Purdue University, West Lafayette, IN 47907, USA

<sup>3</sup>Climate Sciences Department, Climate & Ecosystem Sciences Division, Lawrence Berkeley National  
Laboratory, Berkeley, CA 94720, USA

<sup>4</sup>Department of Earth Sciences, University of Minnesota, Minneapolis, MN, 55455, USA

<sup>5</sup>Institute of Environmental Physics, University of Bremen, Otto-Hahn-Allee 1, Bremen, 28359, Germany

<sup>6</sup>Department of Physics, University of Helsinki, P.O. Box 48, 00014 University of Helsinki, Finland

<sup>7</sup>Department of Forest Sciences, P.O. Box 27, 00014 University of Helsinki, Finland

*Correspondence to:* Qianlai Zhuang([gzhuang@purdue.edu](mailto:gzhuang@purdue.edu))

**Abstract:** Carbon monoxide (CO) plays an important role in controlling the oxidizing capacity of the atmosphere by reacting with OH radicals that affect atmospheric methane (CH<sub>4</sub>) dynamics. We develop a process-based biogeochemistry model to quantify CO exchange between soils and the atmosphere with a 5-minute internal time step at the global scale. The model is parameterized using CO flux data from the field and laboratory experiments for eleven representative ecosystem types. The model is then extrapolated to the global terrestrial ecosystems using monthly climate forcing data. Global soil gross consumption, gross production, and net flux of the atmospheric CO are estimated to be from ~~-197 -180 to -197 -180~~, 34 to 36, and ~~-163 -145 to -145 -163~~ Tg CO yr<sup>-1</sup> (1Tg = 10<sup>12</sup> g), respectively, driven with satellite-based atmospheric CO concentration data during 2000-2013. Tropical evergreen forest, savanna and deciduous forest areas are the largest sinks at 123 Tg CO yr<sup>-1</sup>. Soil CO gross consumption is sensitive to air temperature and atmospheric CO concentration while gross production is sensitive to soil organic carbon (SOC) stock and air temperature. By assuming that the spatially-distributed atmospheric CO concentrations (~128 ppbv) are not changing over time, global mean CO net deposition velocity is estimated to be 0.16-0.19 mm s<sup>-1</sup> during the 20<sup>th</sup> century. Under the future climate scenarios, the CO deposition velocity will increase at 0.0002-0.0013 mm s<sup>-1</sup> yr<sup>-1</sup> during 2014-2100, reaching 0.20-0.30 mm s<sup>-1</sup> by the end of the 21<sup>st</sup> century, primarily due to increasing of temperature. Areas near the equator, Eastern US, Europe and eastern Asia will be the largest sinks due to optimum soil moisture and high temperature. The annual global soil net flux of atmospheric CO is primarily controlled by air temperature, soil temperature, SOC and atmospheric CO concentrations, while its monthly variation is mainly determined by air temperature, precipitation, soil temperature and soil moisture.

## 1. Introduction

Carbon monoxide (CO) plays an important role in controlling the oxidizing capacity of the atmosphere by reacting with OH radicals (Logan et al., 1981; Crutzen, 1987; Khalil & Rasmussen, 1990; Prather et al., 1995; Prather & Ehhalt, 2001). CO in the atmosphere can directly and indirectly influence the fate of critical greenhouse gases such as methane (CH<sub>4</sub>) and ozone (O<sub>3</sub>) (Tan and Zhuang, 2012). Although CO



itself absorbs only a limited amount of infrared radiation from the Earth, the cumulative indirect radiative forcing of CO may be even larger than that of the third powerful greenhouse gas, nitrous oxide (N<sub>2</sub>O, Myhre et al., 2013). Current estimates of global CO emissions from both anthropogenic and natural sources range from 1550 to 2900 Tg CO yr<sup>-1</sup>, which are mainly from anthropogenic and natural direct emissions and from the oxidation of methane and other Volatile Organic Compounds (VOC) (Prather et al., 1995; Khalil et al., 1999; Bergamaschi et al., 2000; Prather & Ehhalt, 2001; Stein et al., 2014). Chemical consumption of CO by atmospheric OH and the biological consumption of CO by soil microbes are two major sinks of the atmospheric CO (Conrad, 1988; Lu & Khalil, 1993; Yonemura et al., 2000; Whalen & Reeburgh, 2001).

Soils are globally considered as a major sink for CO due to microbial activities (Whalen and Reeburgh, 2001; King and Weber, 2007). A diverse group of soil microbes including carboxydrotrophs, methanotrophs and nitrifiers are capable of oxidizing CO (King and Weber, 2007). Annually, 10-25% of total earth surface CO emissions were consumed by soils (Sanhueza et al., 1998; King, 1999a; Chan & Steudler, 2006). Potter et al. (1996) reported the global soil consumption to be from -50.46 to -165.0 Tg CO yr<sup>-1</sup> (~~positive values represent the emissions from soils to the atmosphere~~ negative values represent the uptake from the atmosphere to soil), by using a single-box model over the upper 5 cm of soils. All existing estimates have large uncertainties, ~~and estimates~~ range from -64.046 to -64.016 Tg CO yr<sup>-1</sup> (Sanhueza et al., 1998; King, 1999; Bergamaschi et al., 2000). Similarly, the estimates of CO dry deposition velocities also have large uncertainties; ~~and estimates~~ range from 0 to 4.0 mm s<sup>-1</sup> (here positive values are amount of deposition to soils, King, 1999a; Castellanos et al., 2011). Soils also produce CO mainly via abiotic processes such as thermal- and photo-degradation of organic matter or plant materials (Conrad and Seiler, 1985b; Tarr et al., 1995; Schade et al., 1999; Derendorp et al., 2011; Lee et al., 2012; van Asperen et al., 2015; Fraser et al., 2015; Pihlatie et al., 2016), except for a few cases of anaerobic formation. Photo-degradation is identified as radiation-dependent degradation due to absorbing radiation (King et al., 2012). Thermal-degradation is identified as the temperature-dependent degradation of carbon in the absence of radiation and possibly oxygen (Derendorp et al., 2011; Lee et al., 2012; van Asperen et al., 2015; Pihlatie et al., 2016).

These major soil CO production processes, together with soil CO consumption processes, have not been adequately modeled in global soil CO budget estimates.

To date, most top-down atmospheric models applied a dry deposition scheme based on the resistance model of Wesely (1989). Such schemes provided a wide range of dry deposition velocities (Stevenson et al., 2006). Only a few models (MOZART-4, Emmons et al., 2010; CAM-chem, Lamarque et al., 2012) have extended their dry deposition schemes with a parameterization for CO and H<sub>2</sub> uptake through oxidation by soil microbes following the work of Sanderson et al. (2003), which itself was based on extensive measurements from Yonemura et al. (2000). Potter et al. (1996) developed a bottom-up model to simulate CO consumption and production at the global scale. This model is a single box model, only considers top 5cm depth of soil and does not have explicit microbial factors, which might have underestimated CO consumption (Potter et al., 1996; King, 1999a). Current bottom-up CO modeling approaches are mostly based on a limited number of CO *in situ* observations or laboratory studies to quantify regional and global soil consumption (Potter et al., 1996; Sanhueza et al., 1998; Khalil et al., 1999; King, 1999a; Bergamaschi et al., 2000; Prather & Ehrlert, 2001). To our knowledge, no detailed process-based model of soil-atmospheric exchange of CO has been published in the recent 15 years. One reason is that there is an incomplete understanding of biological processes of uptake (King & Weber, 2007; Vreman et al., 2011; He and He, 2014; Pihlatie et al., 2016). Another reason is that there is lack of long-term CO flux measurements for different ecosystem types to calibrate and evaluate the models. CO flux measurements are mostly from short-term field observations or laboratory experiments (e.g. Conrad and Seiler, 1985a; Funk et al., 1994; Tarr et al., 1995; Zepp et al., 1997; Kuhlbusch et al., 1998; Moxley and Smith, 1998; Schade et al., 1999; King and Crosby, 2002; Varella et al., 2004; Lee et al., 2012; Bruhn et al., 2013; van Asperen et al., 2015). The first study to report long-term and continuous field measurements of CO flux over grasslands using a micrometeorological eddy covariance (EC) method is Pihlatie et al. (2016).

To improve the quantification of the global soil CO budget for the period 2000-2013 and CO deposition velocity for the 20th and 21st centuries, this study developed a CO dynamics module (CODM) embedded in a process-based biogeochemistry model,

229 the Terrestrial Ecosystem Model (TEM) (Zhuang et al., 2003, 2004, 2007). CODM was  
230 then calibrated and evaluated using laboratory experiments and field measurements for  
231 different ecosystem types. The atmospheric CO concentration data from MOPITT (Gille,  
232 2013) were used to drive model simulations from 2000 to 2013. A set of century-long  
233 simulations of 1901-2100 were also conducted using the atmospheric CO  
234 concentrations estimated with an empirical function (Badr & Probert, 1994; Potter et al.,  
235 1996). Finally, the effects of multiple forcings on the global CO consumption and  
236 production, including the changes of climate and atmospheric CO concentrations at the  
237 global scale were evaluated with the model.

238

## 239 **2. Method**

### 240 **2.1 Overview**

241 We first developed a daily soil CO dynamics module (CODM) that considers: (1)  
242 soil-atmosphere CO exchange and diffusion process between soil layers, (2)  
243 consumption by soil microbial oxidation, (3) production by soil chemical oxidation, and  
244 (4) the effects of temperature, soil moisture, soil CO substrate and surface atmospheric  
245 CO concentration on these processes. Second, we used the observed soil temperature  
246 and moisture to evaluate TEM hydrology module and soil thermal module in order to  
247 estimate soil physical variables. Then we used the data from laboratory experiments  
248 and CO flux measurements to parameterize the model using the Shuffled Complex  
249 Evolution (SCE-UA) method (Duan et al., 1993). Finally, the model was extrapolated to  
250 the globe at a 0.5° by 0.5° resolution. We conducted three sets of model experiments to  
251 investigate the impact of climate and atmospheric CO concentrations on soil CO  
252 dynamics: 1) simulations for 2000-2013 with MOPITT satellite atmospheric CO  
253 concentration data; 2) simulations for 1901-2100 with constant atmospheric CO  
254 concentrations estimated from an empirical function and the historical climate data  
255 (1901-2013) and three future climate scenarios (2014-2100); and 3) Eight sensitivity  
256 simulations by changing a) constant CO surface concentrations  $\pm 30\%$ , b) SOC  $\pm 30\%$ , c)  
257 precipitation  $\pm 20\%$  and d) air temperature  $\pm 3^\circ\text{C}$  for each pixel, respectively, while  
258 holding other forcing data as they were, during 1999-2000.

259

## 260 2.2 Carbon Monoxide Dynamics Module (CODM)

261 Embedded in TEM (Figure 1), CODM is mainly driven by: (1) soil organic carbon  
 262 availability based on a carbon and nitrogen dynamics module (CNDM) (Zhuang et al.,  
 263 2003); (2) soil temperature profile from a soil thermal module (STM) (Zhuang et al.,  
 264 2001, 2003); and (3) soil moisture profile from a hydrological module (HM) (Bonan,  
 265 1996; Zhuang et al, 2004). Net exchange of CO between the atmosphere and soil is  
 266 determined by the mass balance approach (net flux = total production – total oxidation –  
 267 total soil CO concentration change). According to previous studies, we separated active  
 268 soils (top 30cm) for CO consumption and production into 1 cm thick layers (King, 1999a,  
 269 1999b; Whalen & Reeburgh, 2001; Chan & Steudler, 2006). Between the soil layers, the  
 270 changes of CO concentrations were calculated as:

$$271 \quad \frac{\partial(C(t,i))}{\partial t} = \frac{\partial}{\partial z} \left( D(t,i) \frac{\partial(C(t,i))}{\partial z} \right) + P(t,i) - O(t,i) \quad (1)$$

272 Where  $C(t,i)$  is the CO concentration in layer  $i$  and at time  $t$ , units are  $\text{mg m}^{-3}$ .  $z$  is the  
 273 depth of the soil, units are m.  $D(t,i)$  is the diffusion coefficient for layer  $i$ , units are  $\text{m}^2 \text{s}^{-1}$ .  
 274  $P(t,i)$  is the CO production rate and  $O(t,i)$  is the CO consumption rate. The units of  
 275  $P(t,i)$  and  $O(t,i)$  are  $\text{mg m}^{-3} \text{s}^{-1}$ .  $D(t,i)$  is calculated using the method from Potter et al.  
 276 (1996), [equations \(2\) to \(4\)](#), which are the functions of soil temperature, soil texture and  
 277 soil moisture. The upper boundary condition is specified as the atmospheric CO  
 278 concentration, which is estimated by an empirical function of latitude (Potter et al., 1996)  
 279 or directly measured by the MOPITT satellite during 2000-2013. The lower boundary  
 280 condition is assumed to have no diffusion exchange with the layer underneath. This  
 281 partial differential equation (PDE) is solved using the Crank-Nicolson method for less  
 282 time-step-sensitive solution.

283 CO consumption was modeled in unsaturated soil pores as:

$$284 \quad O(t,i) = V_{max} \cdot f_1(C(t,i)) \cdot f_2(T(t,i)) \cdot f_3(M(t,i)) \quad (2)$$

285 Where  $V_{max}$  is the [ecosystem](#) specific maximum oxidation rate, ~~which and was~~  
 286 ~~estimated previously estimates ranging~~ from 0.3 to 11.1  $\mu\text{g CO g}^{-1} \text{h}^{-1}$  ~~for different~~  
 287 [ecosystems](#) (Whalen & Reeburgh, 2001).  $f_i$  represents the effects of soil CO

288 concentration  $C(t, i)$ , temperature  $T(t, i)$  and moisture  $M(t, i)$  on CO soil consumption.  
 289 Considering CO consumption as the result of microbial activities, we calculated  
 290  $f_1(C(t, i))$ ,  $f_2(T(t, i))$  and  $f_3(M(t, i))$  in a similar way as Zhuang et al. (2004):

$$291 \quad f_1(C(t, i)) = \frac{C(t, i)}{C(t, i) + k_{CO}} \quad (2.1)$$

$$292 \quad f_2(T(t, i)) = Q_{10}^{\frac{T(t, i) - T_{ref}}{10}} \quad (2.2)$$

$$293 \quad f_3(M(t, i)) = \frac{(M(t, i) - M_{min})(M(t, i) - M_{max})}{(M(t, i) - M_{min})(M(t, i) - M_{max}) - (M(t, i) - M_{opt})^2} \quad (2.3)$$

294 Where  $f_1(C(t, i))$  is a multiplier that enhances oxidation rate with increasing soil CO  
 295 concentrations using a Michaelis-Menten function with a half-saturation constant  $k_{CO}$ ,  
 296 and their values were which previously estimateds ranging from 5 to 51  $\mu\text{l CO l}^{-1}$  for  
 297 different ecosystems (Whalen & Reeburgh, 2001);  $f_2(T(t, i))$  is a multiplier that  
 298 enhances CO oxidation rates with increasing soil temperature using a Q10 function with  
 299  $Q_{10}$  coefficients (Whalen & Reeburgh, 2001).  $T_{ref}$  is the reference temperature, units  
 300 are °C (Zhuang et al., 2004, 2013).  $f_3(M(t, i))$  is a multiplier to estimate the biological  
 301 limiting effect that diminishes CO oxidation rates if the soil moisture is not at an optimum  
 302 level ( $M_{opt}$ ).  $M_{min}$ ,  $M_{max}$  and  $M_{opt}$  are the minimum, maximum and optimum volumetric  
 303 soil moistures of oxidation reaction, respectively. Equation (2.2) will overestimate CO  
 304 consumption at higher temperature because in reality CO consumption will decrease at  
 305 higher temperatures than optimum temperature, while  $f_2$  will keep increasing with rising  
 306 temperature. However, the CO consumption is constrained by CO production, and  
 307 equation (1) is used to represent this constraint.

308 We modeled the CO production rate ( $P(t, i)$ ) as a process of chemical oxidation  
 309 constrained by soil organic carbon (SOC) decay (Conrad and Seiler, 1985; Potter et al.  
 310 1996; Jobbagy & Jackson, 2000; van Asperen et al., 2015):

$$311 \quad P(t, i) = P_r(t, i) \cdot E_{SOC} \cdot C_{SOC}(t) \cdot F_{SOC} \quad (3)$$

312 Where  $P_r(t, i)$  is a reference soil CO production rate which has been normalized to rate  
 313 at reference temperature (production rate at temperature  $(t, i)$  divided by production  
 314 rate at reference temperature), which is affected by soil moisture and soil temperature

(Conrad and Seiler, 1985; van Asperen et al., 2015).  $E_{SOC}$  is an estimated nominal CO production factor of  $3.5 \pm 0.9 \times 10^{-9}$  mg CO m<sup>-2</sup> s<sup>-1</sup> per g SOC m<sup>-2</sup> (to 30 cm surface soil depth) (Potter et al., 1996).  $C_{SOC}(t)$  is a SOC content in mg m<sup>-2</sup>, which is provided by CNDM module in TEM.  $F_{SOC}$  is a constant fraction of top 30cm SOC compared to total amount of SOC, which is 0.33 for shrubland areas, 0.42 for grassland areas and 0.50 for forest areas, respectively (Jobbagy & Jackson, 2000).  $P_r(t, i)$  was calculated as:

$$P_r(t, i) = \exp \left( f_4(M(t, i)) \cdot E_{a_{ref}}/R \cdot \left( \frac{1}{273.15 + PT_{ref}} - \frac{1}{T(t, i) + 273.15} \right) \right) \quad (3.1)$$

$$f_4(M(t, i)) = \frac{PM_{ref}}{M(t, i) + PM_{ref}} \quad (3.2)$$

Where equation (3.1) is derived from Arrhenius equation for chemical reactions and normalized using the reference temperature  $PT_{ref}$ .  $E_{a_{ref}}/R$  is the reference activation energy divided by gas constant  $R$ , units are K.  $f_4(M(t, i))$  is the multiplier that reduces activation energy using a regression approach based on laboratory experiment of moisture influences on CO production (Conrad and Seiler, 1985).  $PM_{ref}$  is the reference volumetric soil moisture, ranging from 0.01 to 0.5 volume/volume (v/v). We assumed thermal-degradation as the main CO producing process due to lack of photo-degradation data and hard to distinguish photo-degradation from observations. In order to reduce the bias from thermal-degradation to total abiotic degradation, the equation (3.1) is parameterized by comparing with total production rate. For instance,  $P_r(t, i)$  calculation can perfectly fit the experiment results in Van Asperen et al., 2015 with proper  $PT_{ref}$  (18°C),  $E_{a_{ref}}/R$  (14000 K) and  $PM_{ref}$  (0.5 v/v).

CO deposition velocity was modeled in the same way as equation (19.1) in Seinfeld, et al. (1998):

$$v_d = -F_{net}/C_{CO,air} \quad (4)$$

Where the  $v_d$  is the CO deposition velocity, units are mm s<sup>-1</sup>;  $F_{net}$  is the model estimated CO net flux rate, units are mg CO m<sup>-2</sup> day<sup>-1</sup>;  $C_{CO,air}$  is the CO surface concentration, units are ppbv.  $C_{CO,air}$  can be MOPITT CO surface concentration data or derived CO surface concentrations using the same method as Potter et al. (1996).

Positive values of  $v_d$  are soil uptakes (depositions from air to soils) and negative values are soil emissions.

### 2.3 Model Parameterization and Extrapolation

The model parameterization was conducted in two steps: 1) Thermal and hydrology modules embedded in TEM were revised, calibrated and evaluated by running model with corresponding local meteorological or climatic data at four representative sites, including boreal forest, temperate forest, tropical forest and savanna (Table 1, site No.1 to 4, Figure 2) to minimize model data mismatch in terms of soil temperature and moisture. 2) CODM module was parameterized by running TEM for observational periods with the corresponding local meteorological or climatic data at each reference site (Table 1, Figure 3), and using the Shuffled Complex Evolution Approach in R language (SCE-UA-R) (Duan et al., 1993) to minimize the difference between simulated and observed net CO flux. Eleven parameters including  $k_{CO}$ ,  $V_{max}$ ,  $T_{ref}$ ,  $Q_{10}$ ,  $M_{min}$ ,  $M_{max}$ ,  $M_{opt}$ ,  $E_{SOC}$ ,  $Ea_{ref}/R$ ,  $PM_{ref}$  and  $PT_{ref}$  were optimized (Table 2). To be noticed,  $F_{SOC}$  was not involved in the calibration process. Parameter priors were decided based on previous studies (Conrad & Seiler, 1985; King, 1999b; Whalen & Reeburgh, 2001; Zhuang et al., 2004). SCE-UA-R was used for site No. 6, 8, 10, 11 (Table 1). Each site has been run 50 times using SCE-UA-R with 10000 maximum loops for parameter ensemble, and all of them reached stable state before the end of the loops. For wetlands, the only available data is from site No.12. We used a trial-and-error method to make our simulated results in the range of observed flux rates, with a 10% tolerance. For tropical sites, since tropical savanna vegetation type is a combination type of tropical forest and grassland in our model, we first used Site No. 13 to set priors to fit the experiment results with a 10% tolerance and then evaluated by running our model comparing with site No.7 results. Site No. 9 and 5 were used to evaluate our model results for temperate forest and grassland. Besides the observed climatic and soil property data, we used ERA-Interim reanalysis data from The European Centre for Medium-Range Weather Forecasts (ECMWF) (Dee et al., 2011), AmeriFlux observed meteorology data (<http://ameriflux.lbl.gov/>) and reanalysis climatic data from Climatic Research Unit (CRU, Harris et al., 2013) to fill the missing

environmental data. To sum up, parameters for various ecosystem types in Table 2 were the final results of our parameterization. Model parameterization was conducted for ecosystem types including boreal forest, temperate coniferous forest, temperate deciduous forest, and grassland using SCE-UA-R. Tropical forest and wet tundra used a trial-and-error method to adjust parameters letting simulation results best fit the lab data. Due to limited data availability, we assumed temperate evergreen broadleaf forest having the same parameters as temperate deciduous forest.

## 2.4 Data Organization

To get spatially and temporally explicit estimates of CO consumption, production and net flux at the global scale, we used the data of land cover, soils, climate and leaf area index (LAI) from various sources at a spatial resolution of 0.5° latitude X 0.5° longitude to drive TEM. The land cover data include potential vegetation distribution (Melillo et al., 1993) and soil texture (Zhuang et al., 2003), which were used to assign vegetation- and texture-specific parameters to each grid cell.

For the simulation of the period 1901-2013, monthly air temperature, precipitation, clouds fraction and vapor pressure data sets from CRU were used to estimate the soil temperature, soil moisture and SOC with TEM (Figure 4). Monthly LAI data from TEM were required to simulate soil moisture (Zhuang et al., 2004). During this period time, we used an empirical function of latitude, which was derived from the observed latitudinal distribution of tropospheric carbon monoxide (Badr and Probert, 1994) to calculate [static](#) CO surface concentrations [s\\_distribution](#) (equation (7), Potter et al., 1996):

$$C_{CO,air} = 82.267856 + 0.8441503L + 1.55934 \times 10^{-2}L^2 + 2.37 \times 10^{-5}L^3 - 2.3 \times 10^{-6}L^4 \quad (5)$$

Where  $C_{CO,air}$  is the derived surface CO concentration (ppbv),  $L$  represents latitude which is negative degrees for southern hemisphere and positive degrees for northern hemisphere. We also used the atmospheric CO data from MOPITT satellite during 2000-2013 (Figure 5). We averaged day-time and night-time monthly mean retrieved CO surface level 3 data (variables mapped on 0.5° latitude X 0.5° longitude grid scales with monthly time step, Gille, 2013) to represent the CO surface



concentration level in each month. The missing pixels were fixed by the average of pixels which had values and were inside 1.5 times of the distance between this missing pixel and the nearest pixel with values. These global mean values shown in Figure 5 do not include ocean surfaces, thus there are differences between our surface CO concentration results and Yoon and Pozzer's report in 2014, which is as low as 99.8ppb. From 2014 to 2100, we used Intergovernmental Panel on Climate Change (IPCC) future climate scenarios from Representative Concentration Pathways (RCPs) climate forcing data sets RCP2.6, RCP4.5 and RCP8.5 (Figure 6). RCP2.6, 4.5 and 8.5 datasets are future climate projections with anthropogenic greenhouse gas emission radiative forcing of  $2.6 \text{ W m}^{-2}$ ,  $4.5 \text{ W m}^{-2}$  and  $8.5 \text{ W m}^{-2}$ , respectively, by 2100. Since RCPs did not have water vapor pressure data, we used the specific humidity and sea level air pressure from the RCPs and elevation of surface to estimate the monthly surface vapor pressure (Seinfeld & Pandis, 1998).

## 2.5 Model Experiment Design

We conducted two sets of core simulations and eight sensitivity test simulations for a historical period. The two core sets of simulations were driven with MOPITT CO surface concentrations data for the period 2000-2013 (experiment E1) and with spatially distributed CO surface concentrations assuming as constant over time estimated from an empirical function of latitude for the period 1901-2100 (experiment E2), respectively. Specifically, in experiment E2 we used the CRU climate forcing for the historical period 1901-2013 and the climate data of RCP2.6, RCP4.5 and RCP8.5 for different future scenarios to examine the responses of CO flux to changing climates. Eight sensitivity simulations were driven with varying different forcing variables while keeping others as they were: 1) with constant CO surface concentrations  $\pm 30\%$ , 2) SOC  $\pm 30\%$ , 3) precipitation  $\pm 20\%$  and 4) air temperature  $\pm 3^\circ\text{C}$  for each pixel, respectively, during 1999-2000 (E3).

## 3. Results

### 3.1 Site Evaluation

Both the magnitude and variation of the simulated soil temperature and moisture from cold areas to warm areas compared well to the observations (Figure. 2). The magnitude of the simulated CO flux is comparable and correlated with the observations ( $r$  is about 0.5,  $p$ -value < 0.001, Figures 3, a2, b2-, c2-, d2). Estimated CO fluxes for different ecosystem types range from -28.4 to 1.7 mg CO m<sup>-2</sup> day<sup>-1</sup>, and the root mean square error (RMSE) between simulation and observation at all sites is below 1.5 mg CO m<sup>-2</sup> day<sup>-1</sup>. RMSE for site No. 7 is bigger than 2.0 mg CO m<sup>-2</sup> day<sup>-1</sup> when compared with transparent chamber observations. For boreal forest site, we only had 8 acceptable points in 1994 and 1996 (Figure 3c2).

### 3.2 Global Soil CO Dynamics During 2000-2013

Using the MOPITT CO surface concentration data during 2000-2013 (E1), the estimated mean soil CO consumption, production and net flux (positive values indicate CO emissions from soils to the atmosphere) are from -19789 to -18097, 34 to 36 and -16345 to -14563 Tg CO yr<sup>-1</sup>, respectively (Figure 7a). Consumption is about 4 times larger than production. The annual consumption and net flux trends follow the atmospheric CO concentration trends (Figure 5b, Figure 7a), with a small interannual variability (<10%). The latitudinal distributions of consumption, production and net fluxes share the same spatial pattern. Around 20°S-20°N and 20-60°N are the largest and second largest areas for production and consumption, while the 45°S-45°N area accounts for nearly 90% of the total consumption and production (Figure 7b, Table 3). The Southern and Northern Hemispheres have 41% and 59% of the total consumption, and 47% and 53% of the total production, respectively (Table 3). The highest rates of consumption and production are located in areas close to the equator, and consumption from areas such as eastern US, Europe and eastern Asia also is high (>-1000 mg m<sup>-2</sup> yr<sup>-1</sup>) (Figure 8a, b). Global soils serve as an atmospheric CO sink (Figure 8c). Some areas, such as western US and southern Australia, are CO sources, all of which are grasslands or experiencing dry climate. Tropical evergreen forests are the largest sinks, consuming 86 Tg CO yr<sup>-1</sup>, and tropical savanna and deciduous forest are second and third largest sinks, consuming a total of 37 Tg CO yr<sup>-1</sup> (Table 4). These three ecosystems account for 66% of the total consumption. Tropical evergreen forests are

also the largest source of soil CO production, producing 16 Tg CO yr<sup>-1</sup>, while tropical savanna has a considerable production of 6 Tg CO yr<sup>-1</sup> (Table 4). Moreover, tropical areas, including forested wetlands, forested floodplain and evergreen forests, are most efficient for CO consumption, ranging from -183 to -138 mg CO m<sup>-2</sup> day<sup>-1</sup>. They are also the most efficient for CO production at over 2 mg CO m<sup>-2</sup> day<sup>-1</sup> (Table 4, calculated by fluxes divided by area).

### 3.3 Global Soil CO Dynamics During 1901-2100

Using the constant CO surface concentration, the estimated global mean CO deposition velocities are 0.16-0.19 mm s<sup>-1</sup> for the period 1901-2013. For the period 2014-2100, deposition velocities are 0.18-0.21, 0.18-0.24 and 0.17-0.31 for RCP2.6, 4.5 and 8.5 scenarios, respectively (Figure 9). During 2014-2100, there are significant trends of increasing ~~deposition velocities consumption, production and net flux~~ for nearly all scenarios (Figure 9). The rates of increasing are 0.0002, 0.0005 and 0.0013 mm s<sup>-1</sup> yr<sup>-1</sup>, and will reach 0.20, 0.23 and 0.30 mm s<sup>-1</sup> by the end of the 21<sup>st</sup> century for the RCP2.6, RCP4.5 and RCP8.5 scenarios, respectively (Figure 9). These increasing trends are similar to air temperature increasing trends (Figure 6a). Global distribution patterns of CO deposition velocity are similar to net flux distribution for the period 2000-2013 but there are significant differences among 1901-2013, RCP2.6, RCP4.5 and RCP8.5 scenarios (Figure 10). Deposition velocities are increasing from RCP2.6 to RCP8.5 and larger than in the historical periods in areas near the equator (Figure 10). Areas near the equator and eastern Asia become big sinks of atmospheric CO, while northeastern US becomes a small source in the 21<sup>st</sup> century (Figure 10). Different vegetation types have a large range of deposition velocity, from 0.008 to 1.154 mm s<sup>-1</sup> (Table 54). The tropical forested wetland, tropical forested floodplain and tropical evergreen forest have top three largest deposition velocity of 1.154, 1.117 and 0.879 mm s<sup>-1</sup>, respectively, while desert, short grasslands, and wet tundra have the smallest deposition velocity 0.008, 0.010 and 0.015 mm s<sup>-1</sup>, respectively.

### 3.4 Sensitivity test

494 Eight sensitivity tests have been conducted for the 1999-2000 period, including  
495 changing atmospheric CO by  $\pm 30\%$ , SOC by  $\pm 30\%$ , precipitation by  $\pm 30\%$  and air  
496 temperature by  $\pm 3^\circ\text{C}$  for each pixel (Table 5). Soil CO consumption is most sensitive  
497 (changing 29%) to air temperature while production is most sensitive (changing up to  
498 36%) to both air temperature and SOC (30%). The net CO fluxes have the similar  
499 sensitivities as consumption. Annual CO consumption, production and net flux follow the  
500 change of air temperature (Table 5). In addition, a 30% change in precipitation will not  
501 lead to large changes in CO flux ( $< 3\%$ ).

502

## 503 4. Discussion

### 504 4.1 Comparison with Other Studies

505 Previous studies estimated a large range of global CO consumption from -16 to -  
506 640 Tg CO yr<sup>-1</sup>. Our estimates are from -19789 to -18097 Tg CO yr<sup>-1</sup> for for 2000-2013  
507 using MOPITT satellite CO surface concentration data. Previous studies also provided a  
508 large range for CO production from 0 to 7.6 mg m<sup>-2</sup> day<sup>-1</sup> (reviewed in Pihlatie et al.,  
509 2016). Our results showed averaged CO production ranging from 0.01 to 2.29 mg m<sup>-2</sup>  
510 day<sup>-1</sup>. Previously reported CO deposition velocities for different vegetation types range  
511 from 0.0 to 4.0 mm s<sup>-1</sup> while our results showed an averaged CO deposition velocity  
512 ranging from 0.006 to 1.154 mm s<sup>-1</sup> for different vegetation types. The large uncertainty  
513 of these estimates is mainly due to a different consideration of the microbial activities,  
514 the depth of the soil, and the parameters in the model. In contrast to the estimates of -  
515 5746 to -1657 Tg CO yr<sup>-1</sup> which were based on top 5 cm soils (Potter et al., 1996), our  
516 estimates considered 30cm soils, just as used in Whalen & Reeburgh (2001). In  
517 addition, we used a thinner layer division (1cm each layer) for diffusion process, and  
518 used the Crank-Nicolson method to solve partial differential equations to avoid time step  
519 influences. We also included the microbial CO oxidation process to remove the CO from  
520 soils and the effects of soil moisture, soil temperature, vegetation type and soil CO  
521 substrate on microbial activities. Our soil thermal, soil hydrology and carbon and

nitrogen dynamics simulated in TEM provided carbon substrate spatially and temporally for estimating soil CO dynamics. Overall, although a few previous studies have examined the long-term impacts of climate, land use and nitrogen depositions on CO dynamics (Chan & Steudler, 2006, Pihlatie et al., 2016), the global prediction of soil CO dynamics still has a large uncertainty.

## 4.2 Major Controls to Soil CO Dynamics

Sensitivity tests indicate that consumption is normally much larger than CO production so that the former will determine the dynamics of the net flux (Table 5). Model being sensitive to air temperature explains the small increasing trends after the 1960s, the significant increasing trend in the 21<sup>st</sup> century and the large sinks over tropical areas (Table 5, Figure 9). SOC did not directly influence CO consumption. For instance, increasing SOC led to an increase in soil CO substrate, implying that more CO in soils can be consumed. To be noticed, ~~the CO oxidation increasing due to CO substrate change is larger than production increasing due to SOC increasing, leading to~~ an extra 18 Tg CO yr<sup>-1</sup> ~~was being~~ taken up from the atmosphere to soils in sensitivity test when SOC increasing by 30% (Table 5), ~~which will be discussed in detail later in~~ [Section 4.3.](#) ~~CO surface~~ concentrations will only influence the uptake rate and soil CO substrate concentrations, thus influencing the soil CO consumption rate.

Annual CO consumption and net flux have a similar correlation coefficient with forcing variables and both are significantly correlated with air temperature, soil temperature SOC and atmospheric CO concentration ( $R > 0.91$  globally, Table 6). Increasing temperature will increase microbial activities, while more SOC will increase soil CO substrate level. Annual CO consumption and net flux have low correlations with annual precipitation and soil moisture, especially at 45°N-45°S ( $R < 0.54$  Table 6). Annual CO production is strongly correlated with annual mean SOC, air temperature and soil temperature ( $R > 0.91$ ), while is less correlated with precipitation, soil moisture and atmospheric CO concentration. Meanwhile, the monthly CO consumption, production and net flux are well correlated with air temperature, soil temperature, precipitation, and soil moisture ( $R > 0.69$  globally Table 6). The soil moisture is significantly influenced by temperature at a monthly time step since increasing

temperature would induce higher evapotranspiration. Monthly CO consumption, production and net flux have low correlations with SOC because it will not change greatly within a month.

The R between annual soil CO consumption and atmospheric CO concentration is 0.91 at the global scale because the atmospheric CO concentration, air temperature, and soil temperature dominate the annual consumption rate. At monthly scale, this R is -0.48 because global atmospheric CO concentrations are high in winter and low in summer while the simulated soil CO consumption shows an opposite monthly variation (Table 6, Figure 11), suggesting that other factors such as precipitation, air temperature, and soil temperature are major controls for monthly CO fluxes.

#### 4.3. Model Uncertainties and Limitations

There are a number of limitations, contributing to our simulation uncertainties. First, due to lacking long-period observational data of CO flux and associated environmental factors, the model parameterization can only be conducted for 4 ecosystem types including boreal forest, temperate coniferous forest, temperate deciduous forest and grassland. Tropical forest calibration is only conducted using a very limited amount of lab experiment data, but tropical areas are hotspots for CO soil-atmosphere exchanges. Besides, tropical forest SOC for top 30cm can be really high according to observations. TEM model may underestimate the top 30cm SOC, which will underestimate production rates, especially in tropical regions. Tropical regions typically have high temperature during the whole year, which may result in overestimation of CO consumption using equation (2.2). The large deviation for tropical savanna (which is mosaic of tropical forest and grassland ecosystems) may be due to using outside air temperature to represent inside air temperature of transparent chamber observations (Varella et al., 2004), and uncertain tropical forest parameterization. Second, we used the conclusion from van Asperen et al. (2015) and only considered the thermal-degradation process for CO production in this study. Photo-degradation process and biological formation process were not considered due to lacking understanding of these processes. Third, the ~~static derived~~ CO surface concentration derived from the empirical function is lower than MOPITT CO surface

concentration, which will lead to ~~underestimation~~ ~~overestimation~~ of CO deposition velocity during 1901-2100. ~~Fourth, f- Fourth, the time step (5min) we used for CO dynamics simulation is still not fine enough even we used Crank-Nicolson method to reduce the influences. From sensitivity test (-in tTable 5) and model test (Tin-table 7), we can notice that 5-minute time step will let the diffusion and consumption in the model is too every sensitive to sudden 30% SOC changes with 5-minute time step. In reality, diffusion and consumption shall ,which should only be slightly influenced by indirect changes of soil CO concentration due to SOC changes. When we used 3--minutes or 1-minute time step, the model responses to SOC changes are increasing started to be reasonable (Table 7). However, we believe Moreover, our model using 5--minute step is is-suitable in this study since SOC varies slightly during the whole global simulation period with only {3% increasing from 1900 to 2013 (-Figure 4d) and ;up to a 4% increase ing- from 2014 to 2100 (-Figure 6g). Our ,and-model test showed there are small tiny-responses to these small amounts of is-much-SOC increasing (Table 7). A finer time step (<1min) should be used to reduce the uncertainty in future works, if computing resources permit.-Fifourth, our model structure still has a large potential to improve. In this study we divided the top 30cm soil into 30 layers (layer thickness  $dz=1\text{cm}$ ), but finer division will increase the accuracy (Figure 12). We chose  $dz=1\text{cm}$  because if  $dz>1\text{cm}$ , the model vertical CO concentration profile will deviate from reality and diffusion process will be influenced significantly. If  $dz<1\text{cm}$ , it will need much more computing time but don't have much improvement compared to  $dz=1\text{cm}$  (Figure 12a-e). We notice that the 30-layer division well represents soil CO concentration profile not only for the days with soil CO net uptake, but also for the days with CO net emission (Figure 12c, f). SixFifth, Michaelis-Menten function (equation 2.1) is used in this model and we notice that  $k_{CO}$  is normally much larger than  $C(t,i)$  in those days of net soil uptake (over ten times larger, Figure 12). However, we can't simplify equation (2.2) to  $f_1(C(t,i)) = \frac{C(t,i)}{k_{CO}}$  since CO concentrations in soils can be larger than in the atmosphere in the days of net emissions and  $C(t,i)$  may be close to  $k_{CO}$ , which may lead to overestimation of CO oxidation (Figure 12f). Finally, although we focused on natural ecosystems in this study, land-use change, agriculture activity, and nitrogen deposition also affect the soil CO consumption and production (King, 2002; Chan & Steudler,~~

2006). For instance, soil CO consumption in agriculture ecosystems is 0 to 9 mg CO m<sup>-2</sup> day<sup>-1</sup> in Brazil (King & Hungria, 2002). We used grass land or forest ecosystem to represent agriculture areas in CODM module. Our future study shall include these processes and factors.

## 5. Conclusions

We analyzed the magnitude, spatial pattern, and the controlling factors of the atmosphere-soil CO exchanges at the global scale for the 20th and 21st centuries using a process-based biogeochemistry model. Major processes include atmospheric CO diffusion into soils, microbial oxidation removal of CO, and CO production through chemical reaction. We found that air temperature and soil temperature play a dominant role in determining annual soil CO consumption and production while precipitation, air temperature, and soil temperature are the major controls for the monthly consumption and production. Atmospheric CO concentrations are important for annual CO consumption. We estimated that the global annual CO consumption, production and net fluxes for 2000-2013 are from -19789 to -18097, 34 to 36 and -16345 to -14563 Tg CO yr<sup>-1</sup>, respectively, when using a MOPITT CO surface concentration data. Tropical evergreen forest, savanna and deciduous forest areas are the largest sinks accounting for 66% of the total CO consumption, while the Northern Hemisphere consumes 59% of the global total. During the 20th century, the estimated CO deposition velocity is 0.16-0.19 mm s<sup>-1</sup>. The predicted CO deposition velocity will reach 0.20-0.30 mm s<sup>-1</sup> in the 2090s, primarily because of increasing air temperature. The areas near the equator, eastern Asia, Europe and eastern US will become the sink hotspots because they have warm and moist soils. This study calls for long-period observations of CO flux for various ecosystem types and projection of atmospheric CO surface concentrations from 1901-2100 to improve future estimates of global soil CO consumption. The effects of land-use change, agriculture activities, nitrogen deposition, photo-degradation and biological formation shall also be considered to improve future quantification of soil CO fluxes.



646 **Acknowledgment**

647         This study is supported through projects funded to Q.Z. by Department of Energy  
648 (DE-SC0008092 and DE-SC0007007) and the NSF Division of Information and  
649 Intelligent Systems (NSF-1028291). The supercomputing resource is provided by  
650 Rosen Center for Advanced Computing at Purdue University. We acknowledge Dr.  
651 Stephen C. Whalen made the observational CO flux data available to this study. We are  
652 also grateful to University of Tuscia (dep. DIBAF), Italy, and their affiliated members, for  
653 their help and the use of their field data.

654 **References:**

- 655 Badr, O., & Probert, S. D.: Carbon monoxide concentration in the Earth's atmosphere. *Applied Energy*,  
656 doi:10.1016/0306-2619(94)90035-3, 1994
- 657 Badr, O., & Probert, S. D.: Sinks and environmental impacts for atmospheric carbon monoxide, *Applied*  
658 *Energy*. doi:10.1016/0306-2619(95)98803-A, 1995
- 659 Bartholemew, G.W., Alexander, M.: Soils as a sink for atmospheric carbon monoxide, *Science* 212, 1389-  
660 1391, doi:10.1126/science.212.4501.1389, 1981
- 661 Bartholomew, G. W., & Alexander, M.: Notes. Microorganisms responsible for the oxidation of carbon  
662 monoxide in soil. *Environmental Science & Technology*. American Chemical Society (ACS),  
663 doi:10.1021/es00099a013, 1982
- 664 Bender, M., & Conrad, R.: Microbial oxidation of methane, ammonium and carbon monoxide, and  
665 turnover of nitrous oxide and nitric oxide in soils, *Biogeochemistry*, Springer Nature,  
666 doi:10.1007/bf00002813, 1994
- 667 Bergamaschi, P., Hein, R., Heimann, M., & Crutzen, P. J.: Inverse modeling of the global CO cycle: 1.  
668 Inversion of CO mixing ratios, *Journal of Geophysical Research: Atmospheres*,  
669 doi:10.1029/1999jd900818, 2000
- 670 Bonan, G.: A Land Surface Model (LSM Version 1.0) for Ecological, Hydrological, and Atmospheric  
671 Studies: Technical Description and User's Guide, UCAR/NCAR, doi:10.5065/d6df6p5x, 1996
- 672 Bourgeau-Chavez, L.L., Garwood, G.C., Riordan, K., Koziol, B.W., Slawski, J.: Development of  
673 calibration algorithms for selected water content reflectometry probes for burned and nonburned  
674 organic soils of Alaska. *Int. J. Wildland Fire* 19, 961e975, doi:10.1071/wf07175, 2012
- 675 Bruhn, D., Albert, K. R., Mikkelsen, T. N., & Ambus, P.: UV-induced carbon monoxide emission from living  
676 vegetation. *Biogeosciences*, Copernicus GmbH, doi:10.5194/bg-10-7877-2013, 2013
- 677 Castellanos, P., Marufu, L. T., Doddridge, B. G., Taubman, B. F., Schwab, J. J., Hains, J. C., ...  
678 Dickerson, R. R.: Ozone, oxides of nitrogen, and carbon monoxide during pollution events over the  
679 eastern United States: An evaluation of emissions and vertical mixing, *Journal of Geophysical Research*  
680 *Atmospheres*, 116(16), doi:10.1029/2010JD014540, 2011
- 681 Chan, A. S. K., & Steudler, P. A.: Carbon monoxide uptake kinetics in unamended and long-term  
682 nitrogen-amended temperate forest soils. *FEMS Microbiology Ecology*, 57(3), 343–354,  
683 doi:10.1111/j.1574-6941.2006.00127.x, 2006
- 684 Conrad, R., & Seiler, W.: Role of Microorganisms in the Consumption and Production of Atmospheric  
685 Carbon Monoxide by Soil. *Appl. Environ. Microbiol.*, 40(3), 437–445. Retrieved from  
686 <http://aem.asm.org/cgi/content/abstract/40/3/437>, 1980
- 687 Conrad, R., & Seiler, W.: Arid soils as a source of atmospheric carbon monoxide, *Geophysical Research*  
688 *Letters*, doi:10.1029/gl009i012p01353, 1982

689 Conrad, R., & Seiler, W.: Characteristics of abiological carbon monoxide formation from soil organic  
 690 matter, humic acids, and phenolic compounds, *Environmental Science & Technology*, American Chemical  
 691 Society (ACS), doi:10.1021/es00142a004, 1985  
 692 Conrad, R., Meyer, O., & Seiler, W.: Role of carboxydobacteria in consumption of atmospheric carbon  
 693 monoxide by soil, *Applied and Environmental Microbiology*, 42(2), 211–215, 1981  
 694 Crutzen, P. J., & Giedel, L. T.: A two-dimensional photochemical model of the atmosphere. 2: The  
 695 tropospheric budgets of anthropogenic chlorocarbons CO, CH<sub>4</sub>, CH<sub>3</sub>Cl and the effect of various NO<sub>x</sub>  
 696 sources on tropospheric ozone, *J. Geophys. Res.*, 88(CII), 6641–6661. doi:10.1029/JC088iC11p06641,  
 697 1983  
 698 Crutzen, P.J.: Role of the tropics in atmospheric chemistry, *The Geophisiology of Amazonia Vegetation*  
 699 *Climate Interaction* (Dickinson RE, ed.), pp 107–131. John Wiley, New York, 1987  
 700 Daniel, J. S., & Solomon, S.: On the climate forcing of carbon monoxide, *Journal of Geophysical*  
 701 *Research-Atmospheres*, 103(D11), 13249–13260. doi:10.1029/98JD00822, 1988  
 702 Dee, D. P., Uppala, S. M., Simmons, A. J., Berrisford, P., Poli, P., Kobayashi, S., ... Vitart, F.: The ERA-  
 703 Interim reanalysis: configuration and performance of the data assimilation system, *Quarterly Journal of*  
 704 *the Royal Meteorological Society*, doi:10.1002/qj.828, 2011  
 705 Dentener, F., Drevet, J., Lamarque, J. F., Bey, I., Eickhout, B., Fiore, A. M., ... Wild, O.: Nitrogen and  
 706 sulfur deposition on regional and global scales: A multimodel evaluation, *Global Biogeochemical*  
 707 *Cycles*, 20(4), doi:10.1029/2005GB002672, 2006  
 708 Derendorp, L., Quist, J. B., Holzinger, R., & Röckmann, T.: Emissions of H<sub>2</sub> and CO from leaf litter of  
 709 *Sequoiadendron giganteum*, and their dependence on UV radiation and temperature, *Atmospheric*  
 710 *Environment*, 45(39), 7520–7524. doi:10.1016/j.atmosenv.2011.09.044, 2011  
 711 Duan, Q. Y., Gupta, V. K., & Sorooshian, S.: Shuffled complex evolution approach for effective and  
 712 efficient global minimization, *Journal of Optimization Theory and Applications*, 76(3), 501–521.  
 713 doi:10.1007/BF00939380, 1993  
 714 Duggin, J. A., & Cataldo, D. A.: The rapid oxidation of atmospheric CO to CO<sub>2</sub> by soils, *Soil Biology and*  
 715 *Biochemistry*, 17(4), 469–474, doi:10.1016/0038-0717(85)90011-2, 1985  
 716 Emmons, L. K., Walters, S., Hess, P. G., Lamarque, J.-F., Pfister, G. G., Fillmore, D., ... Kloster, S.:  
 717 Description and evaluation of the Model for Ozone and Related chemical Tracers, version 4 (MOZART-  
 718 4), *Geoscientific Model Development*, 3(1), 43–67. doi:10.5194/gmd-3-43-2010, 2010  
 719 Fenchel, T., King, G. M., & Blackburn, T. H.: Bacterial biogeochemistry: the ecophysiology of mineral  
 720 cycling, *Bacterial biogeochemistry* (p. 307 pp). doi:10.1016/B978-0-12-415836-8.00012-8, 1988  
 721 Ferenci, T., Strom, T., & Quayle, J. R.: Oxidation of carbon monoxide and methane by *Pseudomonas*  
 722 *methanica*, *Journal of General Microbiology*, 91(1), 79–91. doi:10.1099/00221287-91-1-79, 1975  
 723 Fisher, M. E.: Soil-atmosphere Exchange of Carbon Monoxide in Forest Stands Exposed to Elevated and  
 724 Ambient CO<sub>2</sub> (Doctoral dissertation), 2003

725 Fraser, W. T., Blei, E., Fry, S. C., Newman, M. F., Reay, D. S., Smith, K. A., & McLeod, A. R.: Emission of  
 726 methane, carbon monoxide, carbon dioxide and short-chain hydrocarbons from vegetation foliage under  
 727 ultraviolet irradiation, *Plant, Cell and Environment*, 38(5), 980–989. doi:10.1111/pce.12489, 2015

728 Funk, D. W., Pullman, E. R., Peterson, K. M., Crill, P. M., & Billings, W. D.: Influence of water table on  
 729 carbon dioxide, carbon monoxide, and methane fluxes from Taiga Bog microcosms, *Global Biogeochem.*  
 730 *Cycles*, 8(3), 271–278. doi:10.1029/94gb0122, 1994

731 Galbally, I., Meyer, C. P., Wang, Y. P., & Kirstine, W.: Soil-atmosphere exchange of CH<sub>4</sub>, CO, N<sub>2</sub>O and  
 732 NO<sub>x</sub> and the effects of land-use change in the semiarid Mallee system in Southeastern Australia, *Global*  
 733 *Change Biology*, 16(9), 2407–2419, doi:10.1111/j.1365-2486.2010.02161.x, 2010

734 Gille, J.: MOPITT Gridded Monthly CO Retrievals (Near and Thermal Infrared Radiances) - Version 6  
 735 [Data set], NASA Langley Atmospheric Science Data Center. doi:10.5067/TERRA/MOPITT/DATA301,  
 736 2013

737 Gödde, M., Meuser, K., & Conrad, R.: Hydrogen consumption and carbon monoxide production in soils  
 738 with different properties, *Biology and Fertility of Soils*, 32(2), 129–134, doi:10.1007/s003740000226, 2000

739 Guthrie, P. D.: The CH<sub>4</sub>- CO - OH conundrum: A simple analytic approach, *Global Biogeochemical*  
 740 *Cycles*, doi:10.1029/gb003i004p00287, 1989

741 Hardy, K. R., & King, G. M.: Enrichment of High-Affinity CO Oxidizers in Maine Forest Soil. *Applied and*  
 742 *Environmental Microbiology*, 67(8), 3671–3676, doi:10.1128/AEM.67.8.3671-3676.2001, 2001

743 Harris, I., Jones, P. D., Osborn, T. J., & Lister, D. H.: Updated high-resolution grids of monthly climatic  
 744 observations - the CRU TS3.10 Dataset, *International Journal of Climatology*, doi:10.1002/joc.3711, 2013

745 He, H., & He, L.: The role of carbon monoxide signaling in the responses of plants to abiotic  
 746 stresses, *Nitric Oxide: Biology and Chemistry / Official Journal of the Nitric Oxide Society*, 42, 40–3.  
 747 doi:10.1016/j.niox.2014.08.011, 2014

748 Heichel, G. H.: Removal of Carbon Monoxide by Field and Forest Soils<sup>1</sup>, *Journal of Environment Quality*,  
 749 *American Society of Agronomy*, doi:10.2134/jeq1973.00472425000200040001x, 1973

750 Jobbagy, E. G., & Jackson, R.: The vertical Distribution of soil organic carbon and its relation to climate  
 751 and vegetation, *Ecological Applications*, 10:2(April), 423–436, doi:10.2307/2641104, 2000

752 Jones, R. D., & Morita, R. Y.: Carbon monoxide oxidation by chemolithotrophic ammonium  
 753 oxidizers, *Canadian Journal of Microbiology*, 29(11), 1545–1551, doi:10.1139/m83-237, 1983

754 Khalil, M. A. ., Pinto, J. ., & Shearer, M.: Atmospheric carbon monoxide, *Chemosphere - Global Change*  
 755 *Science*, Elsevier BV, doi:s1465-9972(99)00053-7,1999

756 Khalil, M. A. K., & Rasmussen, R. A.: The global cycle of carbon monoxide: Trends and mass  
 757 balance, *Chemosphere*, 20(1–2), 227–242, doi:10.1016/0045-6535(90)90098-E, 1990

758 King, G. M.: Attributes of Atmospheric Carbon Monoxide Oxidation by Maine Forest Soils, *Appl. Environ.*  
 759 *Microbiol.*, 65(12), 5257–5264, 1999

760 King, G. M.: Characteristics and significance of atmospheric carbon monoxide consumption by soils,  
 761 Chemosphere, 1, 53–63, doi:10.1016/S1465-9972(99)00021-5, 1999a  
 762 King, G. M.: Land use impacts on atmospheric carbon monoxide consumption by soils, Global  
 763 Biogeochemical Cycles, 14(4), 1161–1172, doi:10.1029/2000GB001272, 2000  
 764 King, G. M., & Crosby, H.: Impacts of plant roots on soil CO cycling and soil-atmosphere CO  
 765 exchange, Global Change Biology, 8(11), 1085–1093, doi:10.1046/j.1365-2486.2002.00545.x, 2002  
 766 King, G. M., & Hungria, M.: Soil-atmosphere CO exchanges and microbial biogeochemistry of CO  
 767 transformations in a Brazilian agricultural ecosystem, Applied and Environmental Microbiology, 68(9),  
 768 4480–4485, doi:10.1128/AEM.68.9.4480-4485.2002, 2002  
 769 King, G. M., & Weber, C. F.: Distribution, diversity and ecology of aerobic CO-oxidizing bacteria, Nature  
 770 Reviews, Microbiology, 5(2), 107–118, doi:10.1038/nrmicro1595, 2007  
 771 King, J. Y., Brandt, L. A., & Adair, E. C.: Shedding light on plant litter decomposition: advances,  
 772 implications and new directions in understanding the role of photodegradation, Biogeochemistry, 111(1–  
 773 3), 57–81, doi:10.1007/s10533-012-9737-9, 2012  
 774 Kisselle, K. W., Zepp, R. G., Burke, R. A., De Pinto, A. S., Bustamante, M. M. C., Opsahl, S., ... Viana, L.  
 775 T.: Seasonal soil fluxes of carbon monoxide in burned and unburned Brazilian savannas, Journal of  
 776 Geophysical Research Atmospheres, 107(20), doi:10.1029/2001JD000638, 2002  
 777 Kuhlbusch, T. A., Zepp, R. G., Miller, W. L., & A BURKE, R.: Carbon monoxide fluxes of different soil  
 778 layers in upland Canadian boreal forests, Tellus B. Informa UK Limited, doi:10.1034/j.1600-  
 779 0889.1998.t01-3-00003.x, 1998  
 780 Lamarque, J. F., Emmons, L. K., Hess, P. G., Kinnison, D. E., Tilmes, S., Vitt, F., ... Tyndall, G. K.: CAM-  
 781 chem: Description and evaluation of interactive atmospheric chemistry in the Community Earth System  
 782 Model, Geoscientific Model Development, 5(2), 369–411, https://doi.org/10.5194/gmd-5-369-2012, 2012  
 783 Lee, H., Rahn, T., & Throop, H.: An accounting of C-based trace gas release during abiotic plant litter  
 784 degradation, Global Change Biology, 18(3), 1185–1195, doi:10.1111/j.1365-2486.2011.02579.x, 2012  
 785 Logan, J. A., Prather, M. J., Wofsy, S. C., & McElroy, M. B.: Tropospheric chemistry - A global  
 786 perspective, J. Geophys. Res., doi:10.1029/JC086iC08p07210, 1981  
 787 Lu, Y., & Khalil, M. A. K.: Methane and carbon monoxide in OH chemistry: The effects of feedbacks and  
 788 reservoirs generated by the reactive products, Chemosphere. Elsevier BV, doi:10.1016/0045-  
 789 6535(93)90450-j, 1993  
 790 Luo, M., Read, W., Kulawik, S., Worden, J., Livesey, N., Bowman, K., & Herman, R.: Carbon monoxide  
 791 (CO) vertical profiles derived from joined TES and MLS measurements, Journal of Geophysical Research  
 792 Atmospheres, 118(18), 10601–10613, doi:10.1002/jgrd.50800, 2013  
 793 Moxley, J. M., & Smith, K. A.: Factors affecting utilisation of atmospheric CO by soils, Soil Biology and  
 794 Biochemistry, 30(1), 65–79, doi:10.1016/S0038-0717(97)00095-3, 1998

795 Myhre, G., Shindell, D., Bréon, F. M., Collins, W., Fuglestedt, J., Huang, J., ... & Nakajima, T.:  
796 Anthropogenic and Natural Radiative Forcing. In: *Climate Change 2013: The Physical Science Basis*,  
797 Contribution of Working Group 1 to the Fifth Assessment Report of the Intergovernmental Panel on  
798 Climate Change. Table, 8, 714, 2013

799 Nakai, T., Kim, Y., Busey, R. C., Suzuki, R., Nagai, S., Kobayashi, H., ... Ito, A.: Characteristics of  
800 evapotranspiration from a permafrost black spruce forest in interior Alaska. *Polar Science*, 7(2), 136–148.  
801 doi:10.1016/j.polar.2013.03.003, 2013

802 Philip, R., & Novick, K.: AmeriFlux US-MMS Morgan Monroe State Forest [Data set]. AmeriFlux; Indiana  
803 University, doi:10.17190/AMF/1246080, 2016

804 Pihlatie, M., Rannik, Ü., Haapanala, S., Peltola, O., Shurpali, N., Martikainen, P. J., ... Mammarella, I.:  
805 Seasonal and diurnal variation in CO fluxes from an agricultural bioenergy crop, *Biogeosciences*.  
806 Copernicus GmbH, doi:10.5194/bg-13-5471-2016, 2016

807 Potter, C. S., Klooster, S. A., & Chatfield, R. B.: Consumption and production of carbon monoxide in soils:  
808 A global model analysis of spatial and seasonal variation, *Chemosphere*, 33(6), 1175–1193,  
809 doi:10.1016/0045-6535(96)00254-8, 1996

810 Prather, M., and Ehhalt, D.: Atmospheric chemistry and greenhouse gases. *Climate Change, 2001: The*  
811 *Scientific Basis* (Houghton JT, Ding Y, Griggs DJ, Noguer M, van der Linden PJ, Dai X, Maskell K &  
812 Johnson CA, eds), pp. 239–288, Cambridge University Press, Cambridge, UK, 2001

813 Prather, M., Derwent, R., Ehhalt, D., Fraser, P., Sanhueza, E. and Zhou, X.: Other trace gases and  
814 atmospheric chemistry, *Climate Change, 1994. Radiative Forcing of Climate Change* (Houghton JT, Meira  
815 Filho LG, Bruce J, Hoesung Lee BA, Callander E, Haites E, Harris N & Maskell K, eds), pp. 76–126,  
816 Cambridge University Press, Cambridge, UK, 1995

817 SALESKA, S. R., DA ROCHA, H. R., HUETE, A. R., NOBRE, A. D., ARTAXO, P. E., & SHIMABUKURO,  
818 Y. E.: LBA-ECO CD-32 Flux Tower Network Data Compilation, Brazilian Amazon: 1999-2006, ORNL  
819 Distributed Active Archive Center, doi:10.3334/ORNLDAAAC/1174, 2013

820 Sanderson, M. G., Collins, W. J., Derwent, R. G., & Johnson, C. E.: Simulation of global hydrogen levels  
821 using a Lagrangian three-dimensional model, *Journal of Atmospheric Chemistry*, 46(1), 15–28,  
822 doi:10.1023/A:1024824223232, 2003

823 Sanhueza, E., Dong, Y., Scharffe, D., Lobert, J. M., & Crutzen, P. J.: Carbon monoxide uptake by  
824 temperate forest soils: The effects of leaves and humus layers, *Tellus, Series B: Chemical and Physical*  
825 *Meteorology*, 50(1), 51–58, doi:10.1034/j.1600-0889.1998.00004.x, 1998

826 Schade, G. W., & Crutzen, P. J.: CO emissions from degrading plant matter (II). Estimate of a global  
827 source strength, *Tellus, Series B: Chemical and Physical Meteorology*, 51(5), 909–918,  
828 doi:10.1034/j.1600-0889.1999.t01-4-00004.x, 1999

829 Scharffe, D., Hao, W. M., Donoso, L., Crutzen, P. J., & Sanhueza, E.: Soil fluxes and atmospheric  
830 concentration of CO and CH<sub>4</sub> in the northern part of the Guayana shield, Venezuela, *Journal of*  
831 *Geophysical Research-Atmospheres*, 95(90), 22475–22480, doi:10.1029/JD095iD13p22475, 1990

Seiler, W.: In: Krumbein, W.E. (Ed.), *Environmental Biogeochemistry and Geomicrobiology, Methods, Metals and Assessment*, vol. 3, Ann Arbor Science, Ann Arbor, MI, pp. 773-810, 1987

Seinfeld, J. H., & Pandis, S. N.: *Atmospheric Chemistry and Physics: From Air Pollution to Climate Change*, Atmospheric Chemistry and Physics from Air Pollution to Climate Change Publisher New York NY Wiley 1998 Physical Description Xxvii 1326 p A WileyInterscience Publication ISBN 0471178152, 51, 1–4, doi:10.1080/00139157.1999.10544295, 1998

Stein, O., Schultz, M. G., Bouarar, I., Clark, H., Huijnen, V., Gaudel, A., ... Clerbaux, C.: On the wintertime low bias of Northern Hemisphere carbon monoxide found in global model simulations, *Atmospheric Chemistry and Physics*, 14(17), 9295–9316, doi:10.5194/acp-14-9295-2014, 2014

Stevenson, D. S., Dentener, F. J., Schultz, M. G., Ellingsen, K., van Noije, T. P. C., Wild, O., ... Szopa, S.: Multimodel ensemble simulations of present-day and near-future tropospheric ozone, *Journal of Geophysical Research Atmospheres*, 111(8), doi:10.1029/2005JD006338, 2006

Suzuki, R.: AmeriFlux US-Prr Poker Flat Research Range Black Spruce Forest [Data set], AmeriFlux; Japan Agency for Marine-Earth Science and Technology, doi:10.17190/AMF/1246153, 2016

Tan, Z., & Zhuang, Q.: An analysis of atmospheric CH<sub>4</sub> concentrations from 1984 to 2008 with a single box atmospheric chemistry model, *Atmospheric Chemistry and Physics Discussions*, Copernicus GmbH, doi:10.5194/acpd-12-30259-2012, 2012

Tarr, M. a., Miller, W. L., & Zepp, R. G.: Direct carbon monoxide photoproduction from plant matter, *Journal of Geophysical Research*, 100, 11403, doi:10.1029/94JD03324, 1995

Taylor, J. A., Zimmerman, P. R., & Erickson, D. J.: A 3-D modelling study of the sources and sinks of atmospheric carbon monoxide, *Ecological Modelling*, 88(1–3), 53–71, doi:10.1016/0304-3800(95)00069-0, 1996

van Asperen, H., Warneke, T., Sabbatini, S., Nicolini, G., Papale, D., & Notholt, J.: The role of photo- and thermal degradation for CO<sub>2</sub> and CO fluxes in an arid ecosystem, *Biogeosciences*, 12(13), 4161–4174, doi:10.5194/bg-12-4161-2015, 2015

Varella, R. F., Bustamante, M. M. C., Pinto, A. S., Kisselle, K. W., Santos, R. V., Burke, R. A., ... Viana, L. T.: Soil fluxes of CO<sub>2</sub>, CO, NO, and N<sub>2</sub>O from an old pasture and from native Savanna in Brazil, *Ecological Applications*, 14(4 SUPPL.), doi:10.1890/01-6014, 2004

Vreman, H. J., Wong, R. J., & Stevenson, D. K.: Quantitating carbon monoxide production from heme by vascular plant preparations in vitro, *Plant Physiology and Biochemistry*, 49(1), 61–68, doi:10.1016/j.plaphy.2010.09.021, 2011

Wesely, M. L.: Parameterization of surface resistances to gaseous dry deposition in regional-scale numerical models. *Atmospheric Environment* (1967), Elsevier BV, doi:10.1016/0004-6981(89)90153-4, 1989

Wesely, M., & Hicks, B.: A review of the current status of knowledge on dry deposition. *Atmospheric Environment*, 34, 2261–2282, doi:10.1016/S1352-2310(99)00467-7, 2000

869 Whalen, S. C., & Reeburgh, W. S.: Carbon monoxide consumption in upland boreal forest soils, *Soil*  
870 *Biology and Biochemistry*, 33(10), 1329–1338, doi:10.1016/S0038-0717(01)00038-4, 2001

871 Yonemura, S., Kawashima, S., & Tsuruta, H.: Carbon monoxide, hydrogen, and methane uptake by soils  
872 in a temperate arable field and a forest, *Journal of Geophysical Research*, 105(D11), 14347,  
873 <https://doi.org/10.1029/1999JD901156>, 2000

874 Yoon, J., & Pozzer, A.: Model-simulated trend of surface carbon monoxide for the 2001-2010  
875 decade, *Atmospheric Chemistry and Physics*, 14(19), 10465–10482, doi:10.5194/acp-14-10465-2014,  
876 2014

877 Zepp, R. G., Miller, W. L., Tarr, M. A., Burke, R. A., & Stocks, B. J.: Soil-atmosphere fluxes of carbon  
878 monoxide during early stages of postfire succession in upland Canadian boreal forests, *Journal of*  
879 *Geophysical Research-Atmospheres*, 102(D24), 29301–29311, doi:10.1029/97jd01326, 1997

880 Zhuang, Q., McGuire, A. D., Melillo, J. M., Clein, J. S., Dargaville, R. J., Kicklighter, D. W., ... Hobbie, J.  
881 E.: Carbon cycling in extratropical terrestrial ecosystems of the Northern Hemisphere during the 20th  
882 century: A modeling analysis of the influences of soil thermal dynamics, *Tellus, Series B: Chemical and*  
883 *Physical Meteorology*, 55(3), 751–776, doi:10.1034/j.1600-0889.2003.00060.x, 2003

884 Zhuang, Q., Melillo, J. M., Kicklighter, D. W., Prinn, R. G., McGuire, A. D., Steudler, P. A., ... Hu, S.:  
885 Methane fluxes between terrestrial ecosystems and the atmosphere at northern high latitudes during the  
886 past century: A retrospective analysis with a process-based biogeochemistry model, *Global*  
887 *Biogeochemical Cycles*, 18(3), doi:10.1029/2004GB002239, 2004

888 Zhuang, Q., Melillo, J. M., McGuire, A. D., Kicklighter, D. W., Prinn, R. G., Steudler, P. A., ... Hu, S.: Net  
889 emissions of CH<sub>4</sub> and CO<sub>2</sub> in Alaska: Implications for the region's greenhouse gas budget, *Ecological*  
890 *Applications*, 17(1), 203–212, doi:10.1890/1051-0761(2007)017[0203:NEOCAC]2.0.CO;2, 2007

891 Zhuang, Q., Romanovsky, V. E., & McGuire, A. D.: Incorporation of a permafrost model into a large-scale  
892 ecosystem model: Evaluation of temporal and spatial scaling issues in simulating soil thermal  
893 dynamics, *Journal of Geophysical Research*, 106, 33649, doi:10.1029/2001JD900151, 2001

894 Zhuang, Q., Chen, M., Xu, K., Tang, J., Saikawa, E., Lu, Y., ... McGuire, A. D.: Response of global soil  
895 consumption of atmospheric methane to changes in atmospheric climate and nitrogen deposition, *Global*  
896 *Biogeochemical Cycles*, doi:10.1002/gbc.20057, 2013



897 **Table 1.** Model parameterization sites for thermal and hydrology modules (site No. 1-4) and for CODM module (site No. 5-13)

No.	Site Name	Location	Vegetation	Driving Climate	Observed Data	Source and Comments
1	Poker Flat Research Range Black Spruce Forest (US_PRR)	147°29'W/65°7'N	Boreal Evergreen Needle Leaf Forests	Site Observation & ERA Interim	Soil Temperature and Moisutre of 2011-2014	Suzuki (2016)
2	Morgan Monroe State Forest (US_MMS)	86°25'W/39°19'N	Temperate Deciduous Broadleaf Forests	Site Observation & ERA Interim	Soil Temperature and Moisutre of 1999-2014	Philip and Novick (2016)
3	Santarem, Tapajos National Forest (STM_K83)	54°56'W/3°3'S	Tropical Moist Forest	Site Observation & ERA Interim	Soil Temperature and Moisutre of 2000-2004	SALESKA et al. (2013)
4	Bananal Island Site (TOC_BAN)	50°08'W/9°49'S	Tropical Forest-Savanna	Site Observation & ERA Interim	Soil Temperature and Moisutre of 2003-2006	SALESKA et al. (2013)
5	Eastern Finland (EF)	27°14'E/63°9'N	Boreal Grassland	Site Observation & ERA Interim	CO flux of April-November,2011	Pihlatie et.al. (2016)
6	Viterbo, Italy (VI)	11°55'E/42°22'N	Mediterranean Grassland	Site Observation & ERA Interim	CO flux of August, 2013	van Asperen et al. (2015)
7	Brasilia, Brazil (BB)	47°51'W/15°56'S	Tropical Savanna	Site Observation & CRU	CO flux of October 1999 to July 2001	Varella et al. (2004)
8	Orange County, North Carolina (OC)	79°7'W/35°58'N	Temperate Coniferous Forest	AMF_US-Dk3 2002-2003	CO flux of March 2002 to March 2003	Fisher (2003)
9	Tsukuba Science City, Japan (TSC)	140°7'E/36°01'N	Temperate Mixed Forest	Site Observation & ERA Interim	CO flux of July 1996 to September 1997	Yonemura et. al. (2000)
10	Manitoba, Canada (CBS)	96°44'W/56°09'N	Boreal Pine Forest	Site Observation & AMF_CA-Man	CO flux of June-August, 1994	Kuhlbusch et. al (1998)
11	Scotland, U.K. (SUK)	3°12'W/55°51'N	Temperate Deciduous Forests	ERA Interim 1995	CO flux of 1995	Moxley and Smith (1998)
12	Alaska, USA (AUS)	147°41'W/64°52'N	Boreal wetland	CRU 1991	CO flux of Lab Experiment,1991	Funk et al. (1994)
13	Guayana Shield,Bolivar State,Venezuela (GBV)	62°57'W/7°51'N	Tropical Smideciduous Forest	CRU 1985	CO flux of Lab Experiment,1985	Scharffe et al. (1990)

900 **Table 2.** Ecosystem-specific parameters in the CODM module<sup>a</sup>

Ecosystem Type	$k_{CO}$ ( $\mu l$ $CO\ l^{-1}$ )	$V_{max}$ ( $\mu g\ CO$ $g^{-1}h^{-1}$ )	$T_{ref}$ (°C)	$Q10$ (Unitless)	$M_{min}$ ( $\frac{v}{v}$ )	$M_{max}$ ( $\frac{v}{v}$ )	$M_{opt}$ ( $\frac{v}{v}$ )	$E_{SOC}$	$F_{SOC}$ ( $\frac{g}{g}$ )	$\frac{Ea_{ref}}{R}$ (K)	$PM_{ref}$ ( $\frac{v}{v}$ )	$PT_{ref}$ (°C)
1 Alpine Tundra & Polar Desert	36.00	0.78	4.00	1.80	0.10	1.00	0.55	3.00	0.33	7700	0.25	30.00
2 Wet Tundra	36.00	0.70	4.00	1.80	0.25	1.00	0.55	3.00	0.42	7700	0.25	30.00
3 Boreal Forest	27.34	1.18	9.81	1.60	0.15	0.64	0.53	2.98	0.50	8827	0.35	26.99
4 Temperate Coniferous Forest	42.64	2.15	6.90	1.87	0.02	0.96	0.53	2.86	0.50	8404	0.38	31.52
5 Temperate Deciduous Forest	40.16	2.43	8.54	1.51	0.17	0.81	0.51	2.45	0.50	8801	0.35	37.44
6 Grassland	42.41	0.49	11.27	1.65	0.16	0.82	0.51	3.09	0.42	14165	0.24	12.29
7 Xeric Shrublands	8.00	0.30	4.00	1.50	0.10	1.00	0.55	3.00	0.33	7700	0.25	30.00
8 Tropical Forest	45.00	2.00	4.00	1.50	0.10	1.00	0.55	3.80	0.50	14000	0.50	18.00
9 Xeric Woodland	8.00	0.30	4.00	1.50	0.10	1.00	0.55	3.00	0.50	7700	0.25	30.00
10 Temperate Evergreen Broadleaf Forest	40.16	2.43	8.54	1.51	0.17	0.81	0.51	2.45	0.50	8801	0.35	37.44
11 Mediterranean Shrubland	45.00	1.50	4.00	1.50	0.10	1.00	0.55	3.00	0.33	7700	0.25	30.00
** Largest Potential Value	51.00	11.1	15.00	2.00	0.30	1.00	0.60	3.80	--	15000	0.60	40.00

901 <sup>a</sup>  $k_{CO}$  is the half-saturation constant for soil CO concentration;  $V_{max}$  is the specific maximum CO oxidation rate;  $T_{ref}$  is the reference  
902 temperature to account for soil temperature effects on CO consumption;  $Q10$  is the an ecosystem-specific Q10 coefficient to account for  
soil temperature effects on CO consumption;  $M_{min}$ ,  $M_{max}$ ,  $M_{opt}$  are the minimum, optimum, and maximum volumetric soil moistures of  
oxidation reaction to account for soil moisture effects on CO consumption;  $E_{SOC}$  is an estimated nominal CO production factor, similar as  
Potter et al. (1996) ( $10^{-4}$  mg CO m<sup>-2</sup> d<sup>-1</sup> per g SOC m<sup>-2</sup>);  $F_{SOC}$  is a constant fraction of top 20cm SOC compared to total amount of SOC  
to account for SOC effects on CO production;  $Ea_{ref}/R$  is the is the ecosystem-specific activation energy divided by gas constant to  
account for the reaction rate of production;  $PM_{ref}$  is the reference moisture to account for soil temperature effects on CO production;  
 $PT_{ref}$  is the reference temperature to account for soil temperature effects on CO production

903 **Table 3.** Regional soil CO consumption, net flux and production (Tg CO yr<sup>-1</sup>) during 2000-2013

	South-45S	45S-0	0-45N	45N-North	Global
Consumption	0.22	75.77	91.66	18.90	186.55
Net flux	0.13	59.34	77.17	14.63	151.27
Production	0.09	16.43	14.49	4.27	35.28

904

905

906 **Table 4.** Annual total soil CO consumption, net flux and production in different ecosystems during 2000-2013  
907 (E1) and mean CO deposition velocity in different ecosystems during 1901-2013 (E2)

Vegetation Type	Area (10 <sup>6</sup> km <sup>2</sup> )	Pixels	Consumption (Tg CO yr <sup>-1</sup> )	Net flux (Tg CO yr <sup>-1</sup> )	Production (Tg CO yr <sup>-1</sup> )	Deposition velocity (mm s <sup>-1</sup> )
Alpine Tundra & Polar Desert	5.28	3580	-0.92	-0.69	0.23	0.023
Wet Tundra	5.24	4212	-1.00	-0.42	0.58	0.015
Boreal Forest	12.47	7578	-7.76	-6.01	1.75	0.070
Forested Boreal Wetland	0.23	130	-0.14	-0.09	0.04	0.109
Boreal Woodland	6.48	4545	-2.48	-1.54	0.94	0.036
Non-Forested Boreal Wetland	0.83	623	-0.35	-0.18	0.17	0.029
Mixed Temperate Forest	5.25	2320	-10.49	-9.98	0.51	0.204
Temperate Coniferous Forest	2.49	1127	-3.51	-3.21	0.30	0.185
Temperate Deciduous Forests	3.65	1666	-5.07	-4.83	0.25	0.151
Temperate Forested Wetland	0.15	60	-0.35	-0.35	0.01	0.281
Tall Grassland	3.63	1567	-1.66	-0.65	1.01	0.021
Short Grassland	4.71	2072	-1.05	-0.27	0.78	0.010
Tropical Savanna	13.85	4666	-21.86	-15.88	5.98	0.234
Xeric Shrubland	14.71	5784	-1.95	-1.64	0.31	0.021
Tropical Evergreen Forest	17.77	5855	-85.90	-69.66	16.24	0.879
Tropical Forested Wetland	0.55	178	-3.59	-3.09	0.50	1.154
Tropical Deciduous Forest	4.69	1606	-14.81	-11.78	3.03	0.532
Xeric Woodland	6.85	2387	-8.48	-7.44	1.04	0.246
Tropical Forested Floodplain	0.15	50	-0.89	-0.77	0.12	1.117
Desert	11.61	4170	-0.62	-0.57	0.05	0.008
Tropical Non-forested Wetland	0.06	19	-0.03	-0.02	0.01	0.067
Tropical Non-forested Floodplain	0.36	120	-0.35	-0.24	0.10	0.083
Temperate Non-Forested Weland	0.34	120	-0.33	-0.20	0.14	0.089
Temperate Forested Floodplain	0.10	48	-0.13	-0.12	0.00	0.197
Temperate Non-forested Floodplain	0.10	45	-0.05	-0.03	0.02	0.050
Wet Savanna	0.16	59	-0.39	-0.32	0.07	0.434
Salt Marsh	0.09	35	-0.05	-0.03	0.03	0.035
Mangroves	0.12	38	-0.49	-0.41	0.08	0.809
Temperate Savannas	6.83	2921	-3.83	-3.22	0.61	0.076
Temperate Evergreen Broadleaf	3.33	1268	-7.17	-6.95	0.22	0.252
Mediterranean Shrubland	1.47	575	-0.86	-0.71	0.16	0.100
Total	133.56	59424	-186.55	-151.27	35.28	--

913  
914  
915  
  
916  
917  
918  
919  
920  
921  
922  
923  
924  
925  
926  
927  
928  
929  
930  
931  
932  
933  
934  
935

**Table 5.** Sensitivity of global CO consumption, net flux and production (Tg CO yr<sup>-1</sup>) to changes in atmospheric CO, soil organic carbon (SOC), precipitation (Prec) and air temperature (AT)

	Baseline	CO +30%	CO -30%	SOC +30%	SOC -30%	Prec +30%	Prec -30%	AT +3°C	AT -3°C
Consumption	-147.65	-164.14	-131.12	-175.37	-119.90	-150.72	-143.50	-190.59	-114.83
Change (%)	0.00	-11.17	-11.19	-18.78	-18.79	-2.08	-2.81	-29.09	-22.23
Net flux	-113.65	-130.15	-97.12	-131.18	-96.10	-116.97	-109.32	-144.23	-89.58
Change (%)	0.00	-14.51	-14.54	-15.42	-15.44	-2.92	-3.81	-26.90	-21.18
Production	33.99	33.99	33.99	44.19	23.80	33.74	34.17	46.36	25.25
Change (%)	0.00	0.00	0.00	30.00	-30.00	-0.75	0.53	36.39	-25.72

936

937

938

939

**Table 6.** Correlation coefficients between forcing variables (precipitation (Prec), air temperature (Tair), soil organic carbon (SOC), soil temperature (Tsoil), soil moisture (Msoil) and atmospheric CO (CO air)) and absolute values of consumption, production and net flux for different regions and the globe

		Monthly					Annual				
		North- 45°N	45°N- 0°	0°- 45°S	45°S- South	Global	North- 45°N	45°N- 0°	0°- 45°S	45°S- South	Global
Prec	Consumption	0.91	0.96	0.92	-0.34	0.87	0.65	0.21	0.26	0.13	0.52
	Production	0.91	0.70	0.45	-0.34	0.82	0.63	0.10	0.15	-0.11	0.47
	Net flux	0.91	0.97	0.94	-0.33	0.87	0.65	0.25	0.31	0.32	0.54
Tair	Consumption	0.97	0.98	0.91	0.96	0.95	0.92	0.93	0.88	0.84	0.91
	Production	0.96	0.83	0.72	0.98	0.94	0.92	0.92	0.91	0.95	0.91
	Net Flux	0.97	0.97	0.88	0.90	0.95	0.91	0.92	0.85	0.62	0.91
SOC	Consumption	-0.19	0.07	0.21	-0.01	0.15	0.68	0.90	0.92	0.47	0.92
	Production	-0.19	0.31	0.47	-0.02	0.24	0.72	0.92	0.92	0.50	0.93
	Net Flux	-0.19	0.03	0.14	0.00	0.13	0.67	0.88	0.91	0.38	0.91
Tsoil	Consumption	0.97	0.98	0.92	0.96	0.95	0.94	0.93	0.88	0.85	0.95
	Production	0.97	0.83	0.72	0.98	0.94	0.94	0.92	0.91	0.96	0.95
	Net Flux	0.98	0.97	0.88	0.90	0.95	0.93	0.93	0.86	0.63	0.95
Msoil	Consumption	0.85	0.96	0.92	0.19	0.76	0.03	0.22	0.14	0.26	0.22
	Production	0.85	0.75	0.44	0.14	0.69	-0.02	0.12	0.02	0.05	0.17
	Net Flux	0.84	0.96	0.95	0.25	0.77	0.04	0.26	0.19	0.40	0.24
CO Air	Consumption	-0.66	-0.76	-0.29	0.14	-0.48	0.87	0.88	0.81	0.98	0.91
	Production	-0.70	-0.66	0.08	-0.40	-0.66	-0.36	-0.48	-0.54	-0.44	-0.57
	Net Flux	-0.64	-0.73	-0.35	0.55	-0.41	0.92	0.91	0.88	0.99	0.94

940

941

942

943

944

945

946

947

948

949

950

Table 7. Model test for site No.8 during 2002-2003. Time step ~~is~~ is for solving eqn. 1 ~~what we used in internal~~  
~~loop for CO dynamics simulation.~~ SOC increasing represents ~~the how many~~ percentage of SOC increased in  
~~for each test.~~ Baseline is ~~the model~~ simulation ~~results~~ using original time step and SOC input. Differences  
~~Change value~~ represents new simulation results minus baseline results.

Time Step	SOC Increasing	Units: $\text{mg m}^{-2} \text{yr}^{-1}$	Consumption	Production	Diffusion
5min	0%	Baseline	-1611.5	410.0	-1201.5
	30%	Change	-293.0	123.0	-170.0
5min	30%	ValueDifferences			
	30%	Change	-156.7	123.0	-33.7
3min	30%	ValueDifferences			
	30%	Differences Change	-97.4	123.0	25.6
1min	10%	Value			
	10%	DifferencesChange	-97.7	41.0	-56.7
5min	1%	Value			
	1%	Change	-9.8	4.1	-5.7
5min		ValueDifferences			

Formatted: Indent: First line: 0"

Formatted: Superscript

Formatted: Superscript

Formatted: Indent: First line: 0"

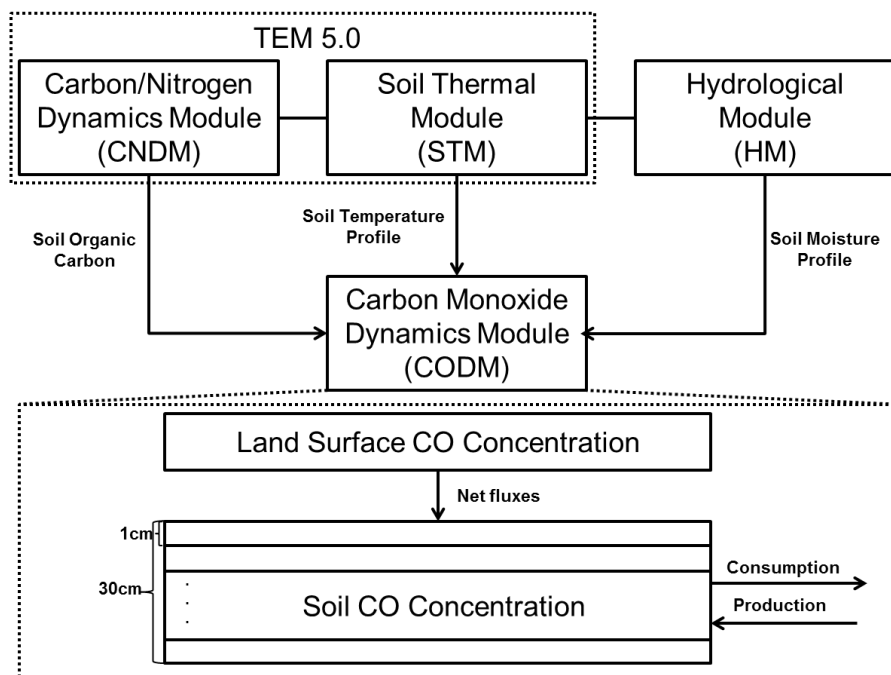


**Figure 1. The model framework** includes a carbon and nitrogen dynamics module (CNDM), a soil thermal module (STM) from Terrestrial Ecosystem Model (TEM) 5.0 (Zhuang et al., 2001, 2003), a hydrological module (HM) based on a Land Surface Module (Bonan, 1996; Zhuang et al., 2004), and a carbon monoxide dynamics module (CODM). The detailed structure of CODM includes land surface CO concentration as top boundary and thirty 1 cm thick layers (totally 30 cm) where consumption and production take place.



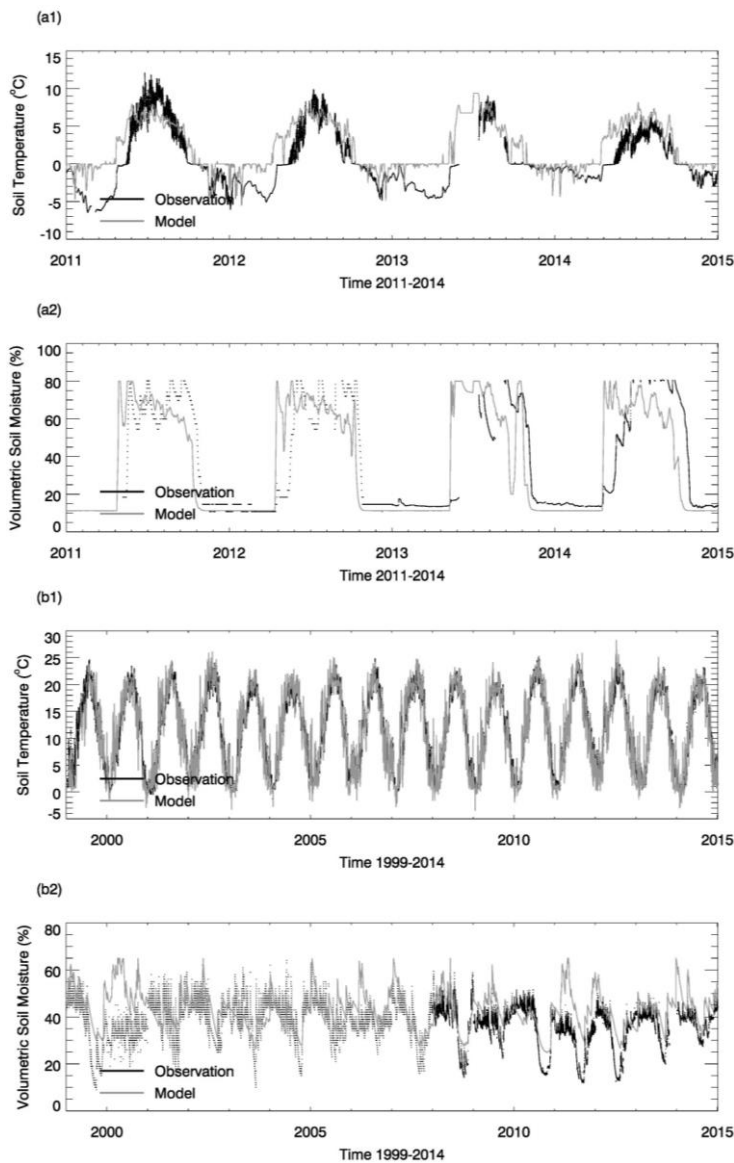


**Figure 2.** Evaluation of thermal and hydrology module at four sites: (a) Boreal Evergreen Needle Leaf Forests, (b) Temperate Deciduous Broadleaf Forests. (1) shows the soil temperature comparison between model simulations (gray line) and observations (black line) and (2) shows the soil moisture comparison between model simulations (gray line) and observations (black line). Specifically, the volumetric soil moisture is converted from the water content reflectometry (WCR) probe output period using an empirical calibration function of Bourgeau-Chavez et al. (2012) for 5cm-30cm layer. Some of them resulted in calculations of values greater than 100% VSM in Nakai et al. (2013) study. Our model estimated high VSM (close to 80%) is due to top 10 cm moss in the model which has a saturation VSM of 0.8

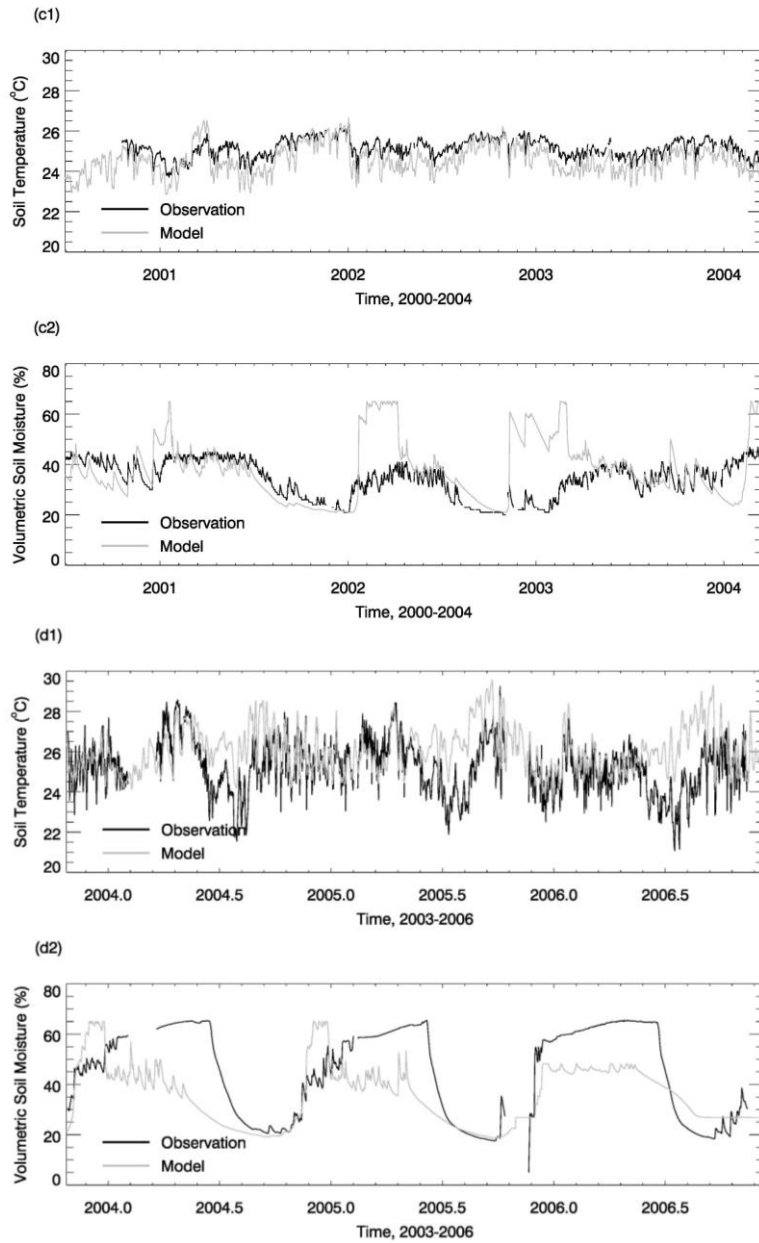
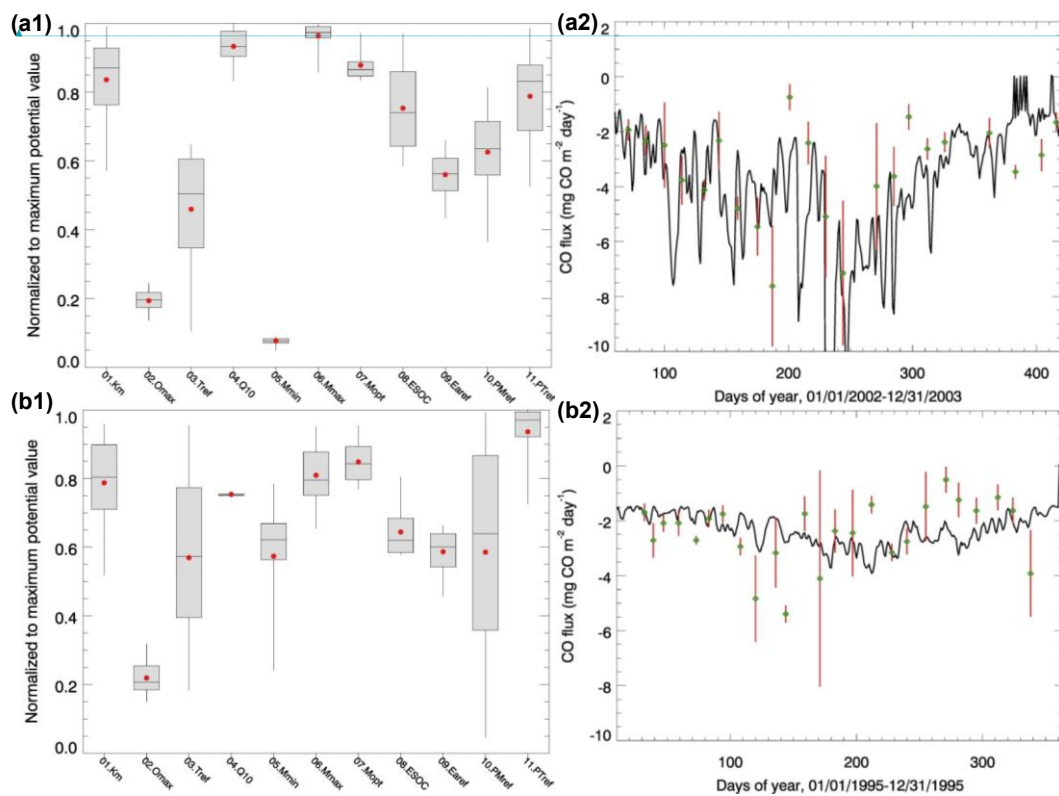


**Figure 2. Contd.** Evaluation of thermal and hydrology module at four sites: (c) Tropical Moist Forest, (d) Tropical Forest-Savanna. (1) shows the soil temperature comparison between model simulations (gray line) and observations (black line) and (2) shows the soil moisture comparison between model simulations (gray line) and observations (black line)



Formatted: Font: (Default) Arial

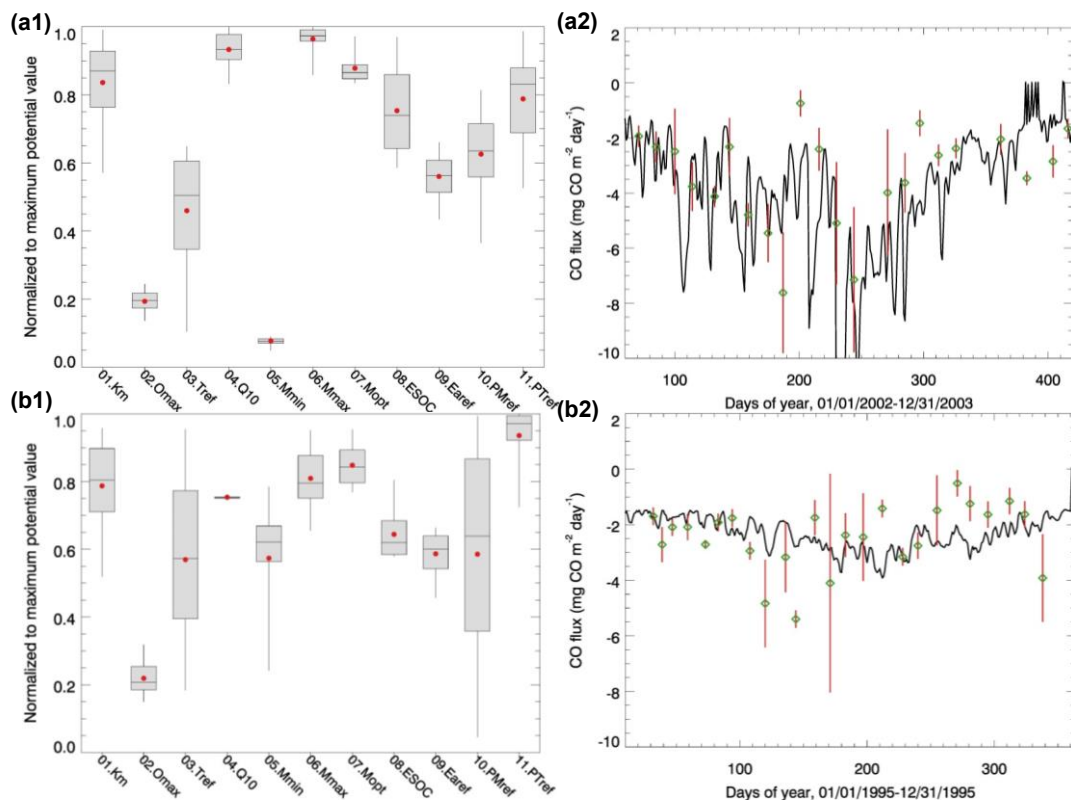
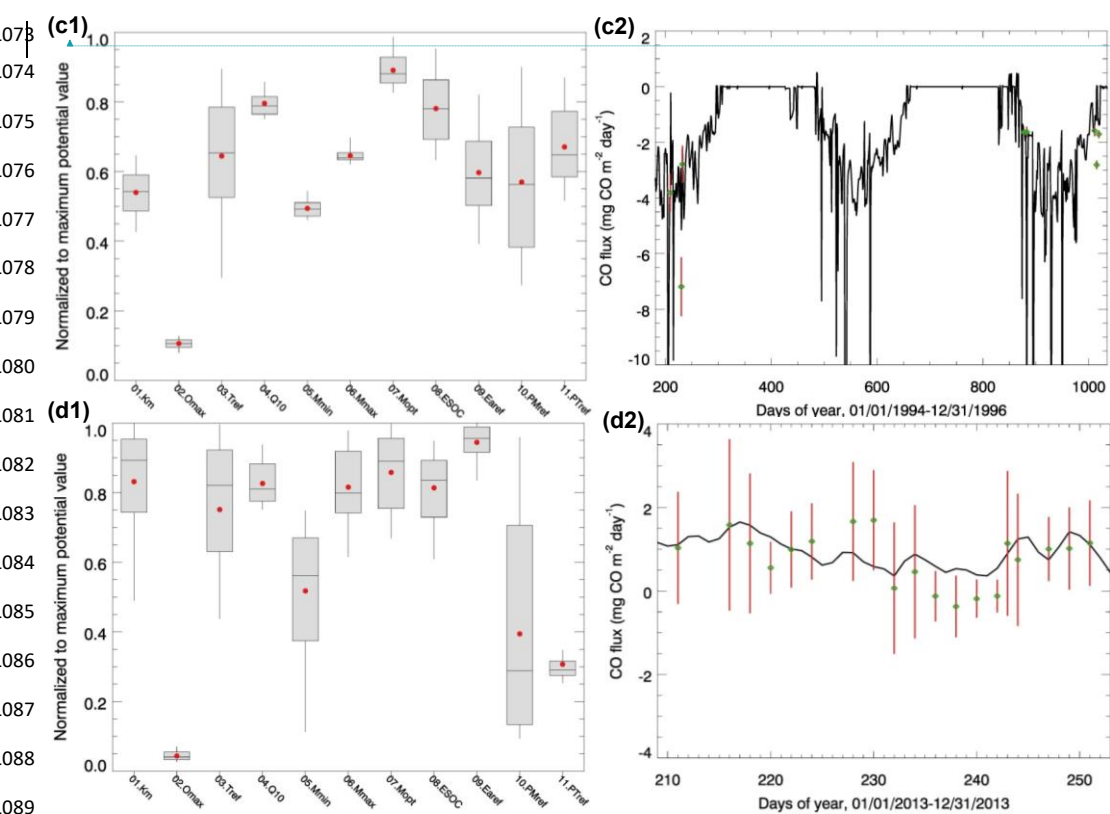


**Figure 3.** Parameter ensemble experiment results: Each parameter has 50 calibrated values generated from running SCE-UA-R 50 times independently. Parameters are normalized to their largest potential values described in Table 2. (a1) and (a2) are temperate coniferous forest normalized parameter distribution boxplots and CO flux comparisons between model simulations (solid line, using mean value of parameters) and observations (green diamond, red lines represent error bar, site No.8), respectively. For each box, line top, box top, horizontal line inside box, box bottom and line bottom represent maximum, third quartile, median, first quartile and minimum of 50 parameter values. Red dot represents the mean value of 50 parameter values. (b1) and (b2) are plots for temperate deciduous forest (site No.11).



Formatted: Font: (Default) Arial

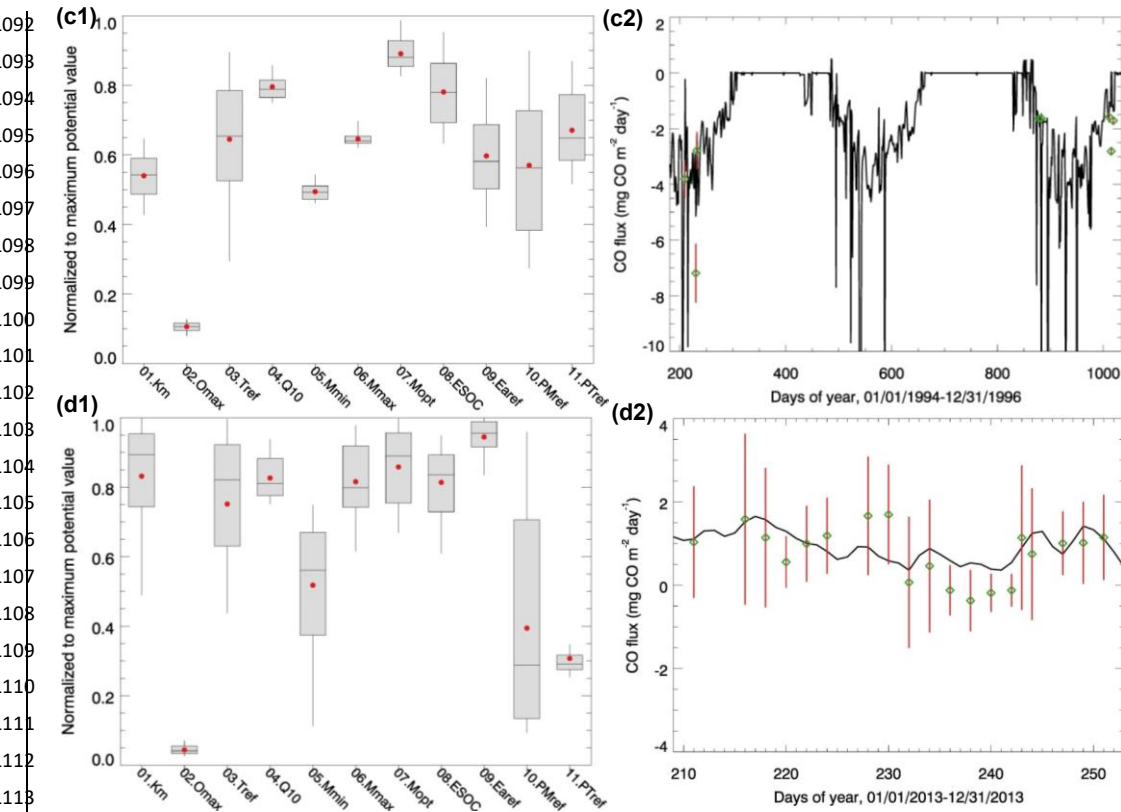


**Figure 3. Contd.** Parameter ensemble experiment results: Each parameter has 50 calibrated values generated from running SCE-UA-R 50 times independently. Parameters are normalized to their largest potential values described in Table 2. (c1) and (c2) are boreal forest normalized parameter distribution boxplots and CO flux comparisons between model simulations (solid line, using mean value of parameters) and observations (green diamond, red lines represent error bar, site No. 12), respectively. For each box, line top, box top, horizontal line inside box, box bottom and line bottom represent maximum, third quartile, median, first quartile and minimum of 50 parameter values. Red dot represents the mean value of 50 parameter values. (d1) and (d2) are for grassland (site No.6). Grassland observation data is the sum of hourly observations so error bar represented the standard deviation.

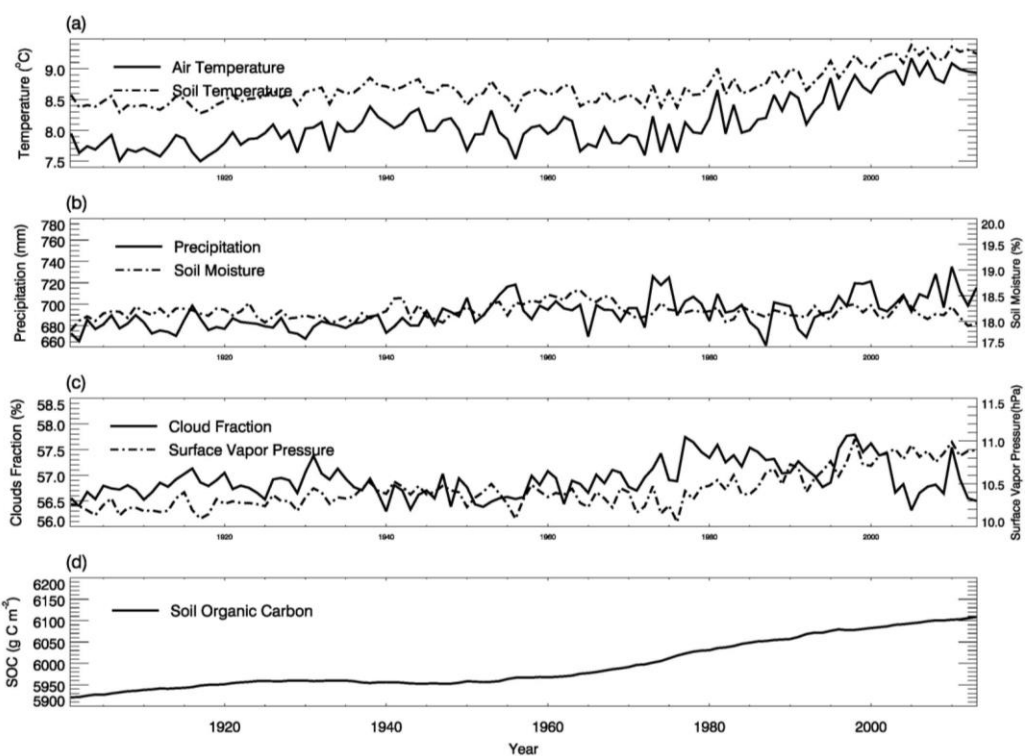


**Figure 4.** Historical global land surface (excluding Antarctic area and ocean area) mean climate, and simulated global mean soil moisture, soil temperature and SOC for the period 1901-2013.

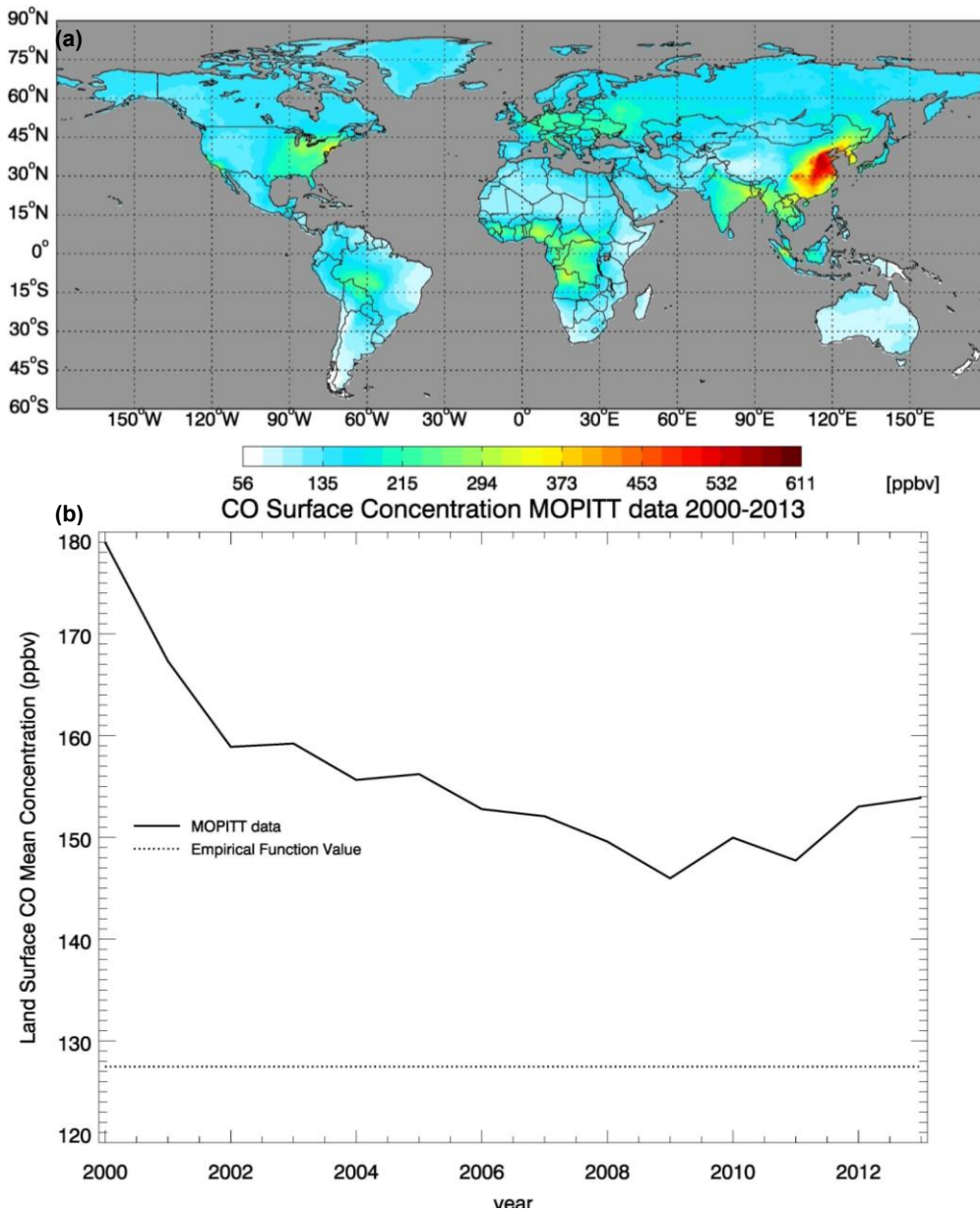


**Figure 5.** CO surface concentration data from MOPITT satellite (ppbv): (a) global mean CO surface concentrations from MOPITT during 2000-2013; (b) the CO annual surface concentrations from both MOPITT and empirical functions (Potter et al., 1996).



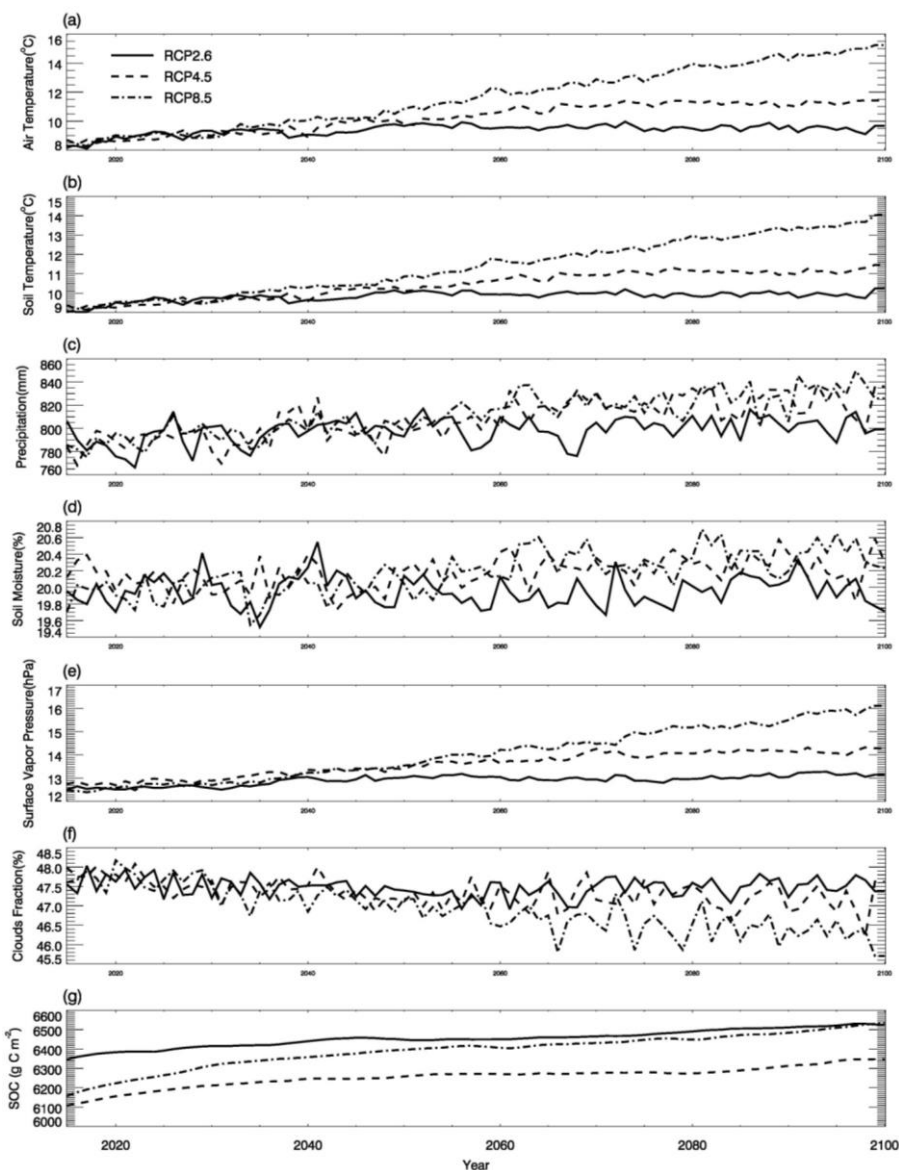


**Figure 6.** Global land surface (excluding Antarctic area and ocean area) mean climate from RCP2.6, RCP4.5 and RCP8.5 data sets and simulated mean soil temperature, moisture and SOC: (a)-(g) are land surface air temperature (°C), soil temperature (°C), precipitation (mm), soil moisture (%), surface water vapor pressure (hpa), cloud fraction (%), and SOC (mg m<sup>-2</sup>), respectively.

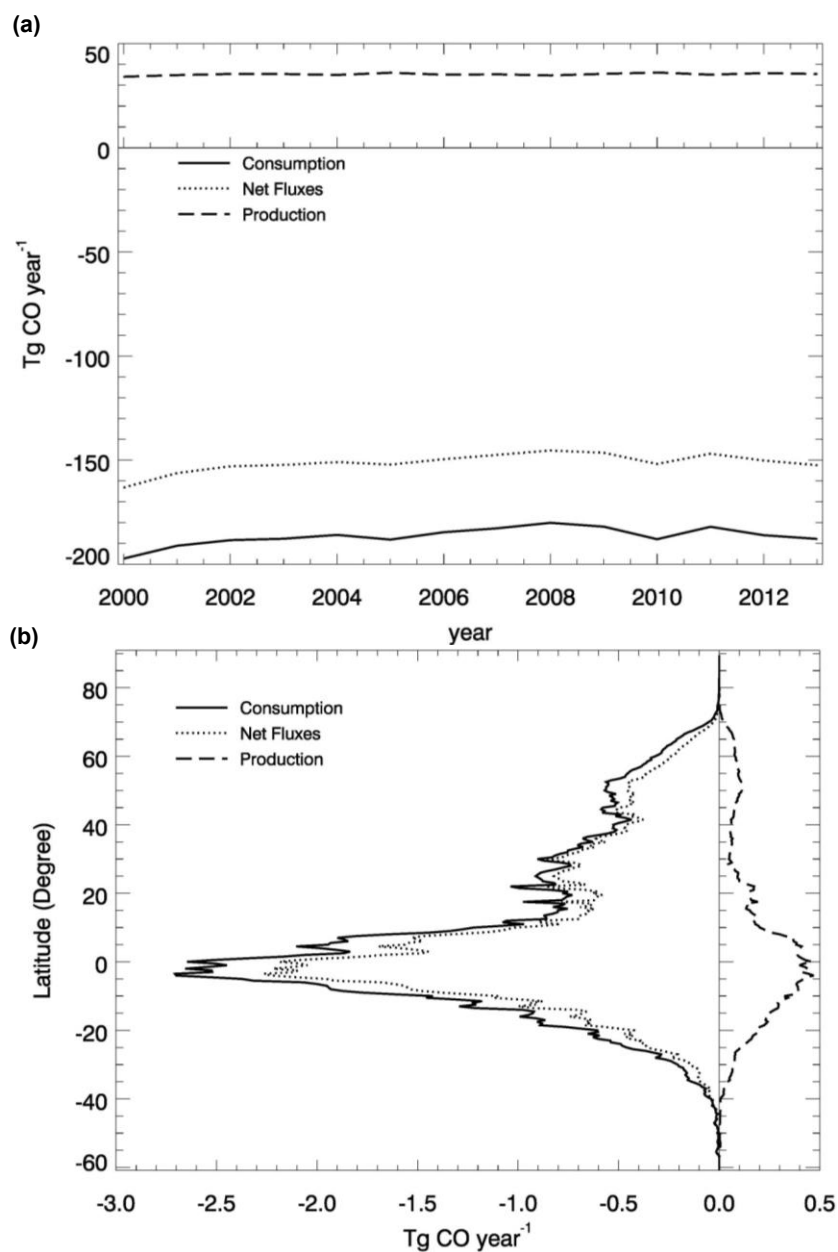


**Figure 7.** Global mean soil CO consumption, production and net flux: (a) annual time series during 2000-2013 and (b) latitudinal distribution during 2000-2013.

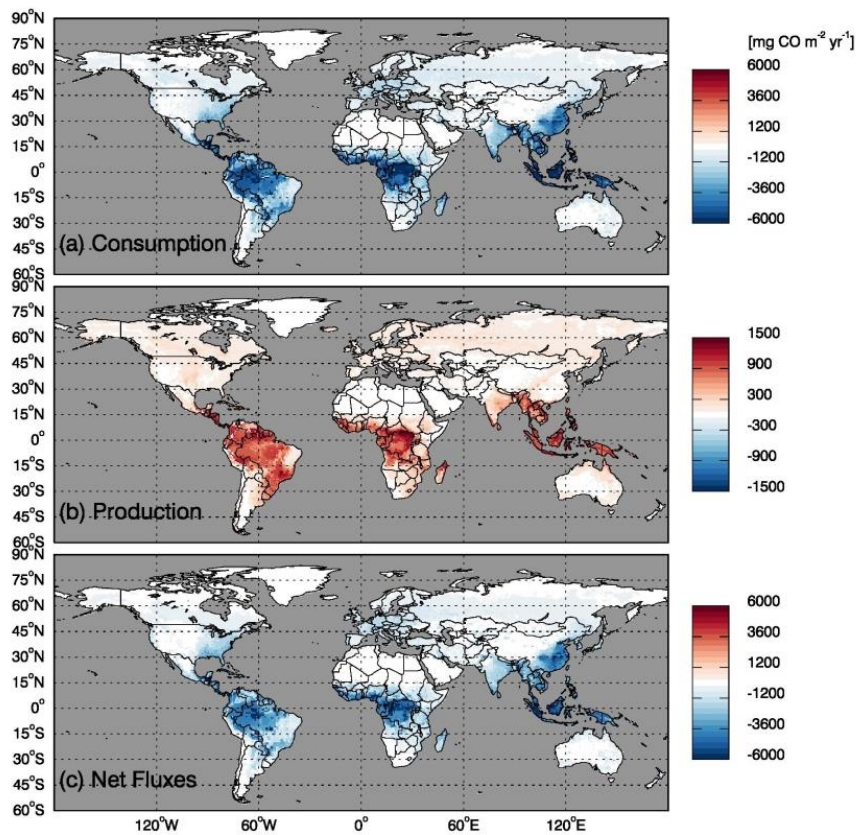


**Figure 8.** Global annual mean soil CO fluxes (mg CO m<sup>-2</sup> yr<sup>-1</sup>) during 2000-2013 using MOPITT CO atmospheric surface concentration data (right side)

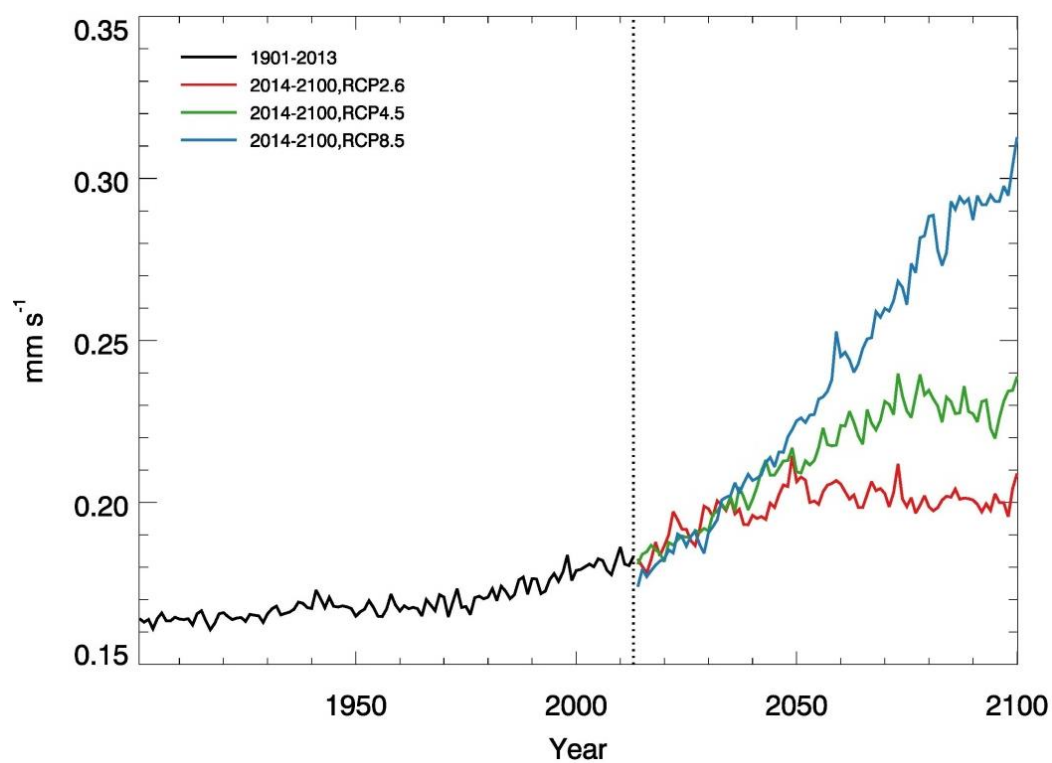


**Figure 9.** [Future](#)-Global mean annual time series of CO deposition velocity (mm s<sup>-1</sup>) using constant in time, spatially distributed CO concentration data during 1901-2013 (left side of dot line) and under future climate scenarios RCP2.6, RCP4.5 and RCP8.5 during 2014-2100 (right side of dot line)

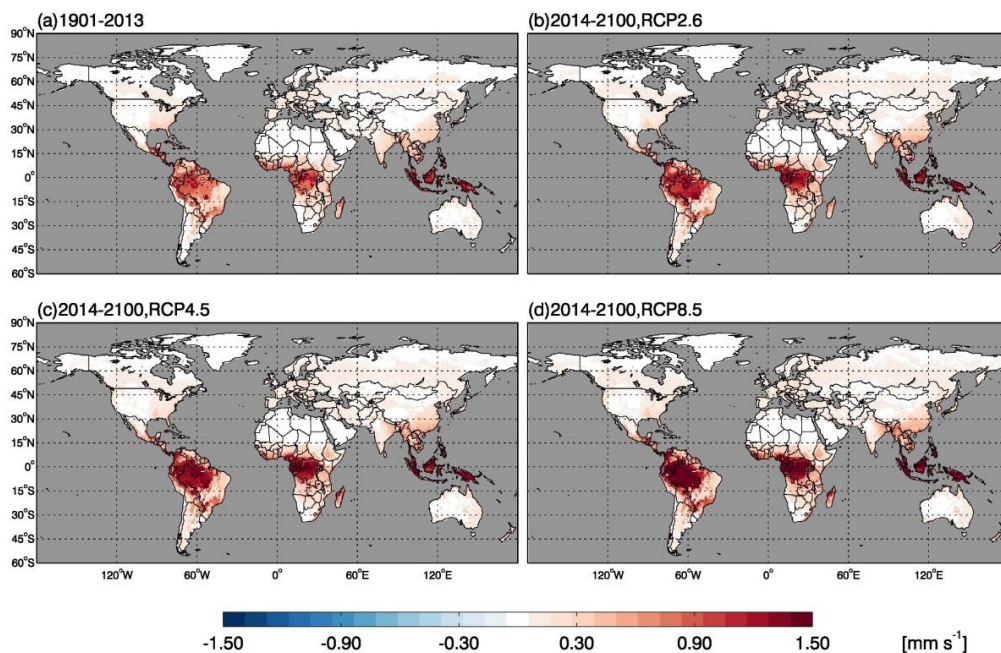


**Figure 10.** Global annual mean CO deposition velocity using constant in time, spatially distributed CO concentration data ( $\text{mm s}^{-1}$ ) a) during 1901-2013 and b), c), d) under future climate scenarios RCP2.6, RCP4.5 and RCP8.5 during 2014-2100, respectively,

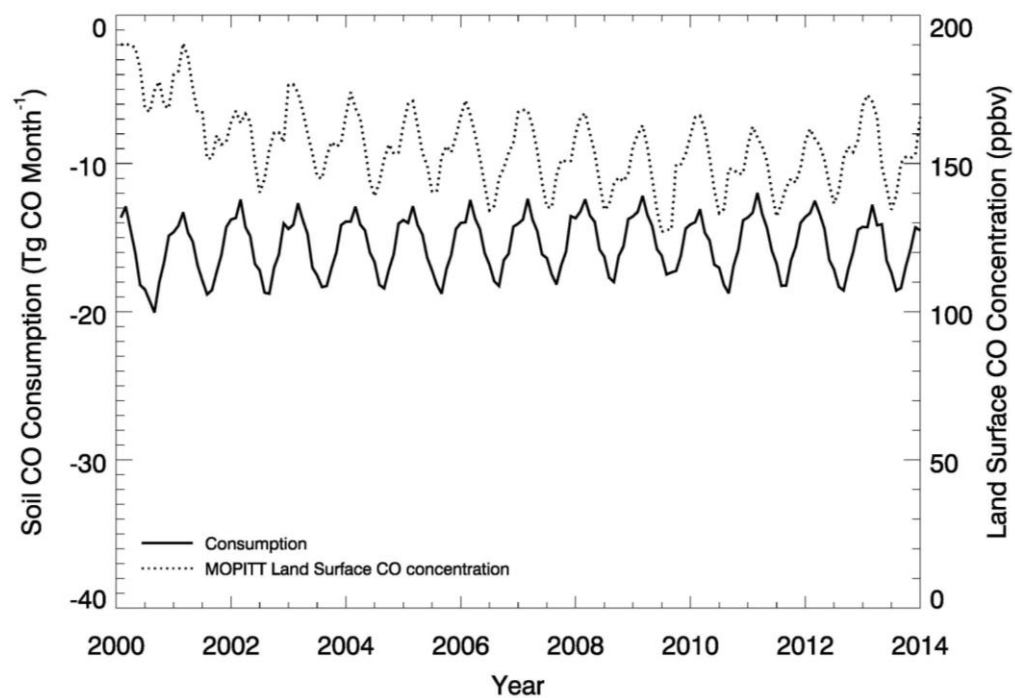
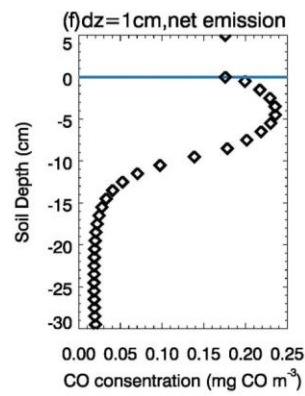
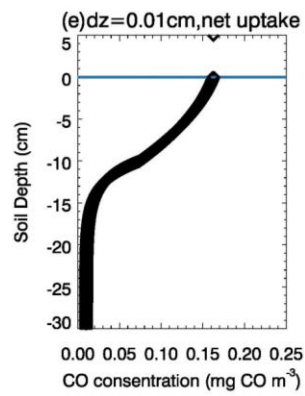
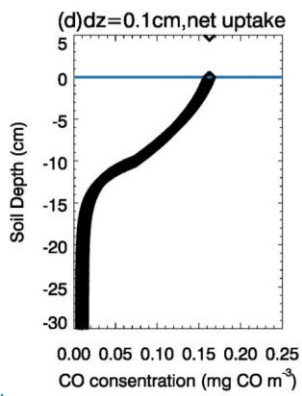
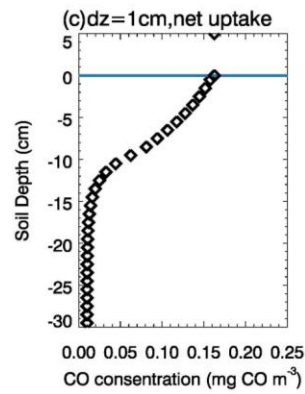
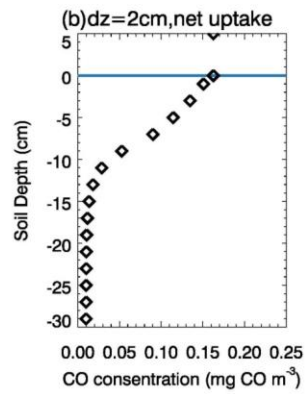
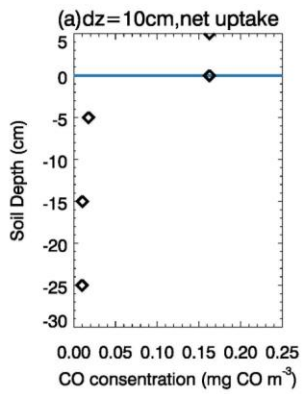


**Figure 11.** Global mean monthly time series of MOPITT surface atmospheric CO concentration (ppbv) and soil CO consumption from model simulations E1 (Tg CO mon<sup>-1</sup>)



Formatted: Font: (Default) Arial, Bold

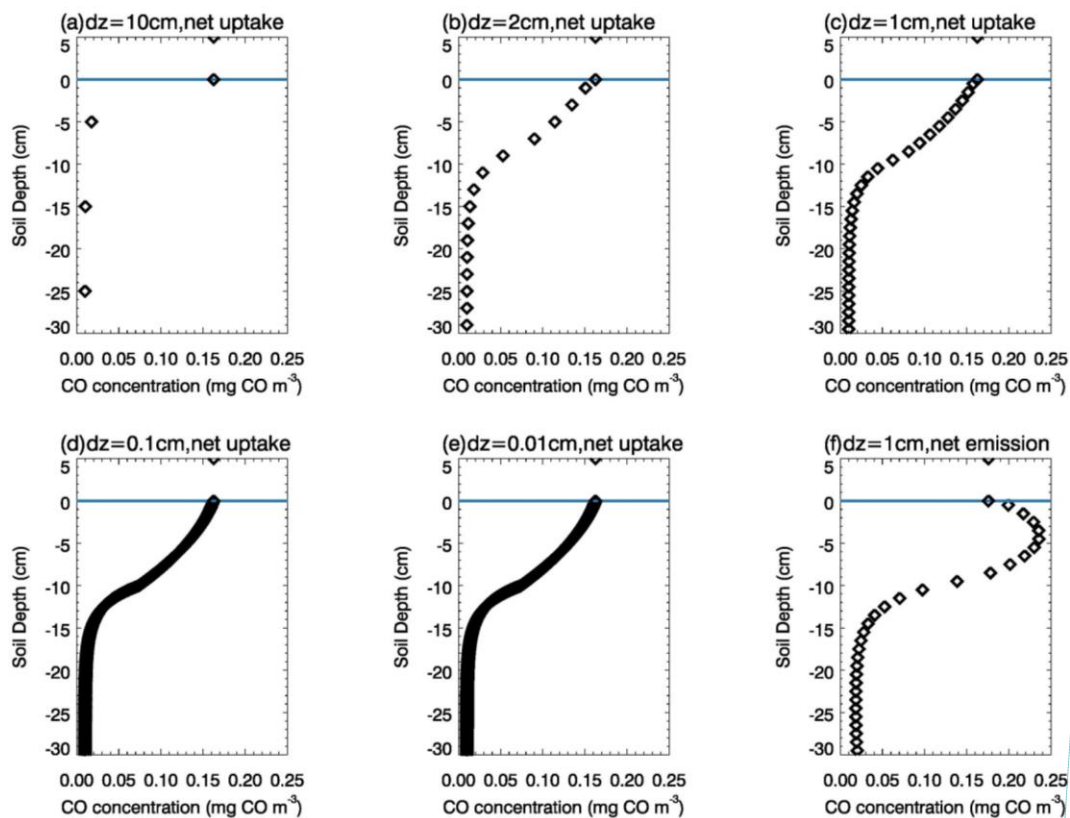


**Figure 12.** Daily mean vertical soil CO concentration profiles of top 30cm. In soils (depth < 0cm), black diamonds represent the soil CO concentration (mg CO m<sup>-3</sup>). Above the surface (depth ≥ 0cm), black diamonds represent atmospheric CO concentration. a), b), c), d) and e) are the results from the same day when soil is a net sink of CO but with different layer thickness ( $dz=10\text{cm}$ ,  $2\text{cm}$ ,  $1\text{cm}$ ,  $0.1\text{cm}$  and  $0.01\text{cm}$  respectively); f) is the result from the day when soil is a net source of CO, with  $dz=1\text{cm}$ .